



Development of a Videographic Pupillometer System for Non-Invasive, Distant Analysis

A Major Qualifying Project Report
Submitted to the Faculty of
WORCESTER POLYTECHNIC INSTITUTE
In partial fulfillment of the requirements for the
Degree of Bachelor of Science

Submitted by:

Harold Hovagimian _____

Christopher Walker _____

Date: **25 April 2012**

Approved by:

Professor Domhnull Granquist-Fraser – Project Advisor

Professor Kristen Billiar – Project Advisor

This report represents work of WPI undergraduate students submitted to the faculty as evidence of a degree requirement. WPI routinely publishes these reports on its web site without editorial or peer review. For more information about the projects program at WPI, see <http://www.wpi.edu/Academics/Projects>.

ABSTRACT

The goal of this project was to develop a remote system capable of obtaining measurements of pupillary diameter of a subject from a distance of two meters. The system was realized by acquiring images using various optical techniques. The analog image data is processed and returns the current pupil diameter and percentage change.

AUTHORSHIP

Both group members contributed equally to this report. The design and development of this device was performed equally by both members, and the workflow was instrumental in the fluidity of process and accomplishment of all tasks and goals set forth in the initial design stages.

ACKNOWLEDGEMENTS

The project team would like to acknowledge Dr. Gregory Blasche of The Charles Stark Draper Laboratory (Cambridge, MA) for supplying us with the radiometer used for eye safety analysis. Additionally, Dr. Blasche provided the team with some initial design components to avoid unnecessary expenditures prior to making final design decisions. Thank you also to Dan Coskren (The Charles Stark Draper Laboratory) Lori Glover (Worcester Polytechnic Institute) and Robert Larsen (The Charles Stark Draper Laboratory) for ensuring that this project succeeded financially. Lastly, this project was supported and guided through the design process in part by the Kristen Billiar (Worcester Polytechnic Institute), Glenn Gaudette (Worcester Polytechnic Institute) and the members of MQP Capstone Design (Worcester Polytechnic Institute, BME430X A11, B11).

The project team would also like to thank the Worcester Polytechnic Institute Biomedical Engineering, Electrical & Computer Engineering and Mechanical Engineering Departments for preparing them to complete this project.

TABLE OF CONTENTS

Abstract	I
Authorship	II
Acknowledgements	III
Table of Contents	IV
Table of Figures	VI
Table of Tables.....	VII
I. Introduction.....	1
II. Background.....	2
2.1 Pupillometry	2
Physiology of the Eye	3
Correlation to Physiological Responses.....	3
Fatigue Detection Based on Infrared Video Pupillography	4
2.2 Active Illumination and The Bright Pupil Effect.....	5
2.3 Optics	7
Telecentric Lens	7
2.4 Data Acquisition.....	8
2.5 Image Processing.....	9
2.6 Potential Artifacts.....	11
Ocular Microtremor.....	11
Head/Body Movement	12
III. Problem Statement	13
Project Goal.....	13
IV. Design Methodology.....	14
4.1 Client Statement and Design Goals.....	14
4.2 Experimental Design	17
4.3 Conceptual Design	19
Image Capture Device - Camera	20
Optical Input Control - Lenses	21
Light Filtering - Optics.....	21
Pupil Illumination Source.....	22
Cabling	23
V. The Remote Pupillometer – Overview	24
5.1 Block Diagram Overview.....	24
Image Acquisition	25
Illumination Circuit.....	25
Data ACQUISITION.....	27
Computer Processing.....	28
VI. Results & Discussion	34
Noise Floor.....	34
Frame Rate	36
Pupillometry Algorithm Error Rate.....	36
Fatigue Analysis.....	38
VII. Recommendations.....	39
VIII. Conclusion.....	41
IX. References	42
X. Appendices	44
Appendix A: Product Datasheets	44
Midwest Optical Systems Inc BP850.....	44

Sony Co. XC-EI50	46
Computar TEC-55	50
Osram Opto Semiconductors Inc SFH-4550.....	51
Osram Opto Semiconductors Inc SFH-4058.....	58
Osram Opto Semiconductors Inc SFH-4250-z.....	66
BitFlow Inc CAB-DEV-ANV1	75
BitFlow-MATLAB IMAQ Integration Properties	77
Newport 1830C with Silicon Detector	85
Appendix B: Safety Hazards Report	87
Appendix C: MATLAB Code Used for Image Processing and Analysis	88
Pupillometry.m	88
pupilProcess.m	91
eliminateReflections.M	94
LSellipse_fit.m	96
Appendix D: MATLAB Code Profiles	99
pupilProcess.m	100
eliminateReflections.m.....	101
LSellipse_fit.m	102

TABLE OF FIGURES

Figure 1: Flowchart of the procedure used for Automatic Pupillometry (Iskander, 2004).....	10
Figure 2: Objectives Tree	15
Figure 3: High-Level System Block Diagram.....	24
Figure 4: Illumination Source	26
Figure 5: Outer Ring Schematic	27
Figure 6: High-Level Software Flow Diagram of Pupillometry.m	29
Figure 7: Software Flow Diagram for pupilProcess.m	30
Figure 8: Original Image Input to Pupillometry.m for Processing	31
Figure 9: Histogram of Pixel Intensity of a Sample Image with No Other Reflections	32
Figure 10: Comparison of Images Between Pupillometry Algorithm Processes	33
Figure 11: Plot of Noise Level Testing Data (1-Minute Duration)	35
Figure 12: Output Image Following Processing with Eyeglass Impairments	38

TABLE OF TABLES

Table 1: Pairwise Comparison Chart: Overall Design Objectives	17
Table 2: Pairwise Comparison Chart: Sub-objective (Useful).....	18
Table 3: Pairwise Comparison Chart: Sub-objective (Stand-alone)	18
Table 4: Pairwise Comparison Chart: Sub-objective (Marketable)	19
Table 5: Noise Level Testing Data (One-Minute Duration)	35
Table 6: Algorithm Error Rate with and Without Reflections	37

I. INTRODUCTION

The analysis of human biometrics has progressed extensively over the past 10 years. Furthermore, as technological advancement continues, applications pertinent to this area of study will continue to arise. In this area, there is a growing need for a method to non-invasively and unobtrusively analyze the level of fatigue of a human subject. This technology would have applications within almost every industry (e.g. safety, productivity, and clinical assessment).

This project aimed to achieve this function by monitoring the change in pupil diameter over time. Through correlation to experimental data, the detection of fatigue could be possible through these means.

II. BACKGROUND

Specific changes in pupil diameter have been correlated with various physiological states and responses; however, there is no system that is currently commercially available to collect and analyze this data from a remote distance from the subject. The following section will provide detailed information regarding pupillometry, human physiological phenomena specific to this application, and information regarding the general operation of an optical measurement system.

2.1 PUPILLOMETRY

The measurement and/or recording of pupil area or diameter as a function of time is known as pupillometry [Fried, 1980]. The pupil reacts and changes due to external (e.g. bright ambient light flash) [Lowenstein, 1963] and internal/physiological (e.g. cognitive function) stimuli [Bolger, 2000]. In medical applications, pupillometry is used for pupillary assessment pre- and post- operatively, diagnostics and proper fitting of glasses and contacts. Pupillometry has also become an effective, non-invasive method to measure fatigue and toxicology, in addition to applications involving behavior science and screening for ophthalmic procedures [Essam, 2010]. The technology has progressed rapidly, and presently can achieve accuracy within 0.1mm [Iskander, 2004]. Furthermore, the current devices used to complete these assessments have become relatively inexpensive, and can provide data analysis within 15-30 seconds.

These devices provide means to analyze subjects in various environments (e.g. clinical); however, the device must perform a measurement in close proximity to the subject. Therefore, the subject is likely aware that the measurements are being taken. In specific applications, it is imperative that the subject be unaffected by the devices' normal operation or the device must operate at a distance from the subject. By analyzing the subject remotely, the device would not interfere with the subjects' duties and tasks and this non-invasive and non-intrusive method allows for subject assessment and analysis without impairment, whereas current market devices would distract a subject from normal activity. Therefore, the goal of this project is to expand on the currently available pupillometry technology to develop a device that operates remotely from the subject. Additionally, the physical envelope the device will be designed to operate in will be minimized to reduce potential interference and interruption during normal device operation.

PHYSIOLOGY OF THE EYE

The pupil is the black hole located in the center of the eye that allows light to enter the retina and is innervated by the autonomic central nervous system. The pupillary diameter is controlled by the iris, which determines the amount of light allowed into the retina. The pupil will dilate or constrict based on different stimuli such as visible light intensity or emotional stimuli.

The diameter of the pupil is controlled by stimulation and relaxation of the sphincter pupillae and dilator pupillae by the sympathetic and parasympathetic innervation. The pupil dilates in response to low light conditions, extreme emotional situations such as desire, pain or fear, certain drugs such as cocaine or amphetamines and other stimuli. The pupil constricts in response to fewer stimuli, but some examples are in response to bright visible light and certain drugs such as alcohol or morphine.

The eyes move rapidly at all times, known as a saccadic movement, scanning the environment and creating a three dimensional map of the environment. [Cassin, 1990] The attention to this movement is necessary when looking at potential artifacts and potential noise, as it may potentially cause skewed results and cause image analysis leg.

CORRELATION TO PHYSIOLOGICAL RESPONSES

As previously stated, the reason for using spontaneous pupillary fluctuation to measure physiological condition is because these responses are innervated by autonomic nervous system whose activity is known to change in parallel with drowsiness and typically cannot be influenced by subjective motive of people. The only manner in which the pupillary dilation may be voluntarily controlled is when the subject imagines an event or object, which would evoke pupil dilation. [Whipple, 1992] Using this established alertness parallelism and eliminating the potential for subject influence, measuring the pupillary diameter is a clear choice for physiological fatigue.

Physiological fatigue is a loss of maximal force generating capacity during muscular activity or a failure of the functional organ. It may be induced by excessive energy consumption; or the depletion of hormones, neurotransmitters or essential physiological substrates. Physiological fatigue may be associated with fever, infection, anemia, sleep disturbances, and

pregnancy. Psychological fatigue, in contrast, has been defined as a state of weariness related to reduced motivation. Psychological fatigue has been associated with stress and other intense emotional experiences and may accompany depression and anxiety. [Siegle, 2004]

The pupil diameter oscillates in all living persons. An analysis of the pupil of an alert and non-drowsy subject shows an oscillation with low amplitude, rarely exceeding $\pm 5\%$. [Lowenstein, 1963] In contrast, the pupil of a drowsy or fatigued subject will fluctuate in diameter with large amplitude at low frequencies. This project will use analysis of the amplitude and frequency of the diameter fluctuation.

The results show that significant differences can be found in drowsy and alert groups: in the drowsy group, pupil diameter fluctuates with large amplitude at low frequencies; while in the alert group pupil size remains stable for a long time and oscillating with amplitudes rarely exceeding $\pm 5\%$ (about 0.3mm).

FATIGUE DETECTION BASED ON INFRARED VIDEO PUPILLOGRAPHY

There exists a gap between the potential capabilities and applications and the functionality of devices currently commercially available. Various products have been developed to obtain measurements and utilize algorithms to correlate the measurements with conditions, such as the alertness (or alternatively, fatigue) level of a subject. However, no commercially available system has succeeded in meeting the requirements of completing high-accuracy measurements remotely with a system that is lightweight and inexpensive.

The FIT® System, developed by PMI, Inc., is used to assess the fitness-for-duty of military soldiers. Additionally, the device can be used for impairment screening. The device weighs 19 pounds, which allows for, but does not optimize, portable use. Scientific validation performed by reputable research organizations has concluded that the device has a 0.022 mm pupil measurement resolution. Despite these advantageous specifications, the device cannot complete measurements remotely, and therefore, would interfere with the behavioral tasking of the subject. [PMI Incorporated, 2011].

Many pupillometer devices have been developed for use by opticians to assess a subject's need for corrective or preventative ophthalmic procedures. Accuracy and repeatability is the most important characteristic for a device with this application, because, in some instances, an intraocular lens (IOL) lens implant is created to the size specified by the measurement device. To

maximize accuracy, these devices, such as the Procyon P3000 (list price of approximately \$7,000) and the Colvard pupillometer (list price of approximately \$2,000), operate in from a distance of less than 0.2 m from the subject. In terms of operation, while the Procyon P3000 measures the pupil diameter changes to known changes in light stimulus, the Colvard pupillometer only operates in a dark room setting.

Current pupillometer devices have achieved certain advantageous, marketable functions and features; however, the devices lack the ability to obtain measurements without being located in close proximity to the subject. This requirement inhibits the ability for the device to obtain physiological measurements without constraining the ability for the subject to complete a task. This characteristic is necessary for further applications of pupillometry to be developed. Once this objective has been developed, verified, and validated, algorithms can be implemented to derive conclusions based upon physiological activity.

2.2 ACTIVE ILLUMINATION AND THE BRIGHT PUPIL EFFECT

Pupillometry can be conducted with active or no active illumination. At short distances, no active illumination pupillometry is often utilized. This method is used for observation of the subjects' pupils in various research and diagnostics settings, however this method is limited in range and can be effected by ambient light changes (pupillary light reflex) [Laeng, 2012].

The remote pupillometer device proposed herein was designed to utilize active illumination and investigate the effect on intensity of the illumination source. Using an active illumination source increases the operating range drastically. An active illumination source creates what is known as the bright-pupil effect, where the light that is transmitted through the lens onto the retina is reflected back and the light that is blocked by the pupil is not, creating a bright circle. The eye is a retroreflector, which means that it returns incident light rays back to the source, much like a corner cube. [So, 2002] The phenomenon of retroreflection in the eye is often seen in cat's eyes or red-eye in photographs. [Snyder, 1975] [Smolka, 2003]

When choosing a wavelength for the illumination source, considerations were made regarding intensity, duration and wavelength. The two former considerations will be addressed in the safety analysis, while the effect of wavelength will be explored here. Because light is shined at the eye, the wavelength is a concern when choosing a source to avoid pupillary constriction

interference. The visible range of the eye is approximately 390 to 750nm, so when investigating the wavelength, two important factors of note are retinal absorption and optimal reflection. Previous research has measured the spectral absorption of the retinal pigment epithelium and choroid for humans and found that the percentage absorption at the wavelength interval for the relevant near-infrared region (850-950 nm) is below 30% and decreases linearly with the wavelength. [Geeraets, 1968]

Different wavelengths (frequencies) of light display varying reflection by the retina [Vitabile, 2010]. This is exhibited by measuring the percentage of retinal reflection at varying wavelengths of light. At 950 nanometers (nm), the retina reflects approximately 40% of the source; however, at 850nm, with the light direction directly on the optical axis, 90% of the incident light is reflected. In order for the bright pupil phenomenon to be exhibited, it is imperative that the light direction coincides with the optical axis.

A previously developed system utilized this phenomenon to isolate the pupil during image acquisition. By utilizing two cameras, operating at differing wavelengths of 850nm and 950nm, the system was able to acquire two different images based on the percentage of retinal reflection. By subtracting the image produced at 850nm from the image at 950nm, the system produced an image that included only the light reflected by the retina.

A study conducted by Karlene Nguyen and colleagues at the IBM Almaden Research Center regarding the bright pupil effect have concluded there is a large variation in bright pupil response among human subjects. Findings have shown that there are significant differences in the distribution of rods and cones in the human eye, which may explain this variation [Roorda, 1999]. Additionally, the study concluded that diet and age do not contribute to this variation; however, factors such as average pupil size and iris color may play a role in the bright pupil effect. This finding was noted as a major factor to consider during the implementation of software algorithms.

Using this knowledge of the physiology of the eye, combined with the spectral response of the camera (see Appendix A: Product Datasheets), the optimal wavelength was chosen to be 850 nm.

The safety of the proposed illumination sources for use in the device was examined to ensure that no physical damage could be caused to any direct or indirect user. The safety study and all relevant calculations and conclusions can be found in Appendix B: Safety Hazards

Report. A radiometer (see Appendix A: Product Datasheets) was used to confirm that the calculated values for the safety were consistent with those actually measured. The team acquired a Newport 1830-C radiometer (Newport Corp, Irvine, CA) to measure the spectral irradiance at 850 nm.

2.3 OPTICS

Whether using analog or digital cameras as the image acquisition device, the optics attached to that device becomes a key component to the quality of the image and the data extrapolated from those images. In the design of this device, the calculations rely on the reproducibility of the image under various conditions. To ensure the reliability of the input image, the lens and filter choice are key components of the design.

TELECENTRIC LENS

Perspective and magnification variation due to change in focus are typically seen challenges in a variety of optics applications. A variety of approaches to solutions of this problem have been proposed, but the most effective approach is constant magnification, which is accomplished by telecentric optics. [Wantanabe, 1997]

Optical filtering and limitations of the image acquisition device were utilized to improve the image clarity, reproducibility, and reliability of images prior to processing and analysis. An 850 nm bandpass filter (Midwest Optical Systems Inc., Palatine, IL) was used to isolate the light retroreflected off of the eye (and potentially reflected off other objects within the image space). Through this method, visible light, such as a common room light or flashlight, would not hinder image processing by possessing variable intensity and size. Additionally, the image acquisition device had a relative response curve as a function of wavelength, which pass all wavelengths of light in the range of 400nm to 1000nm; however, each wavelength had a different relative response (see Appendix A: Product Datasheets). The optical filtering eliminated all wavelengths outside the spectrum of interest, and the attenuation rate (approximately 0.3 relative response at

850nm) allowed for distinguishing between retroreflection off of the pupil and reflection off of another object in the image space (e.g. eyeglass frames) through image processing.

2.4 DATA ACQUISITION

An analog-to-digital converter (ADC) is an electronic device that converts a continuous voltage or current to a discrete number proportional to the magnitude of the input to the device. This conversion is necessary for computer analysis of an analog signal, because a computer operates using digital values. Therefore, the ADC samples the analog signal at a specific frequency, known as the sampling rate, to obtain values that can be interpolated to recreate the continuous signal. For recreation of the original signal, it is necessary to sample at a rate that is greater than twice the highest frequency component of the signal being sampled. This requirement is known as the Nyquist Sampling Theorem. If Nyquist frequency is not satisfied during sampling, aliasing, or the representation of a signal at a different frequency, will occur. An anti-aliasing filter is vital for analog-to-digital conversion, and is used to prevent aliasing by filter the frequencies above half of the sampling rate.

The accuracy of the ADC is governed by various properties of the device, which include the resolution and response type. Most analog-to-digital converters operate linearly, and therefore the output of the ADC will have a linear relationship to its input. However, other ADCs possess a logarithmic response, which can be appropriate for certain applications. The resolution of the device, which is typically expressed in bits, describes the number of discrete values that it can output over a range of analog input values. The values produced by the ADC are stored in binary form, and therefore the number of output values is expressed by a value that is a power of two. The number of voltage intervals is given by the following formula:

Number of voltage intervals = 2^M , where M is the resolution of the ADC is bits

Given the number of voltage intervals, the resolution Q of the ADC in terms of voltage or current can be calculated using the following equation:

$$Q = \frac{E_{FSR}}{N} \quad (1)$$

Where E_{FSR} is the full-scale input voltage range and N is the number of voltage intervals (calculation shown, above)

Quantization error is the amount of error incurred during conversion of the analog signal to a discrete value. This error is expressed in percentage, based on the least significant bit. For instance, a twelve-bit ADC has a quantization error of $1/4096$ or 0.024%. Additionally, the physical hardware components of the ADC are subject to imperfections, which will cause the device to deviate from its desired linear response. This error will decrease the resolution of the ADC; however, this error can be decreased or eliminated through calibration.

Specific to image processing, a frame grabber is used, which operates as an ADC. However, the frame grabber must complete analog-to-digital conversion for every pixel of the input image. Therefore, each pixel is quantized, and the image can be represented digitally on a computer screen by plotting each pixel quantity.

2.5 IMAGE PROCESSING

Many different algorithms have been produced to locate the pupil within an image, determine the center of the pupil, and calculate the diameter of the pupil. There are various procedures to perform the intermediate steps of the process, and many complete pupillometry algorithms use a combination of the existing algorithms (or develop new algorithms to complete the same tasks). The software algorithm that has been developed will greatly impact the overall effectiveness and accuracy of the proposed system, and therefore, it is of great importance that the Team allocates an extensive amount of time for its development, debugging, and optimization. Figure 4, below, outlines the steps of the procedure of by a team of engineers of the Contact Lens and Visual Optics Laboratory, School of Optometry at the Queensland University of Technology (Brisbane, Australia).

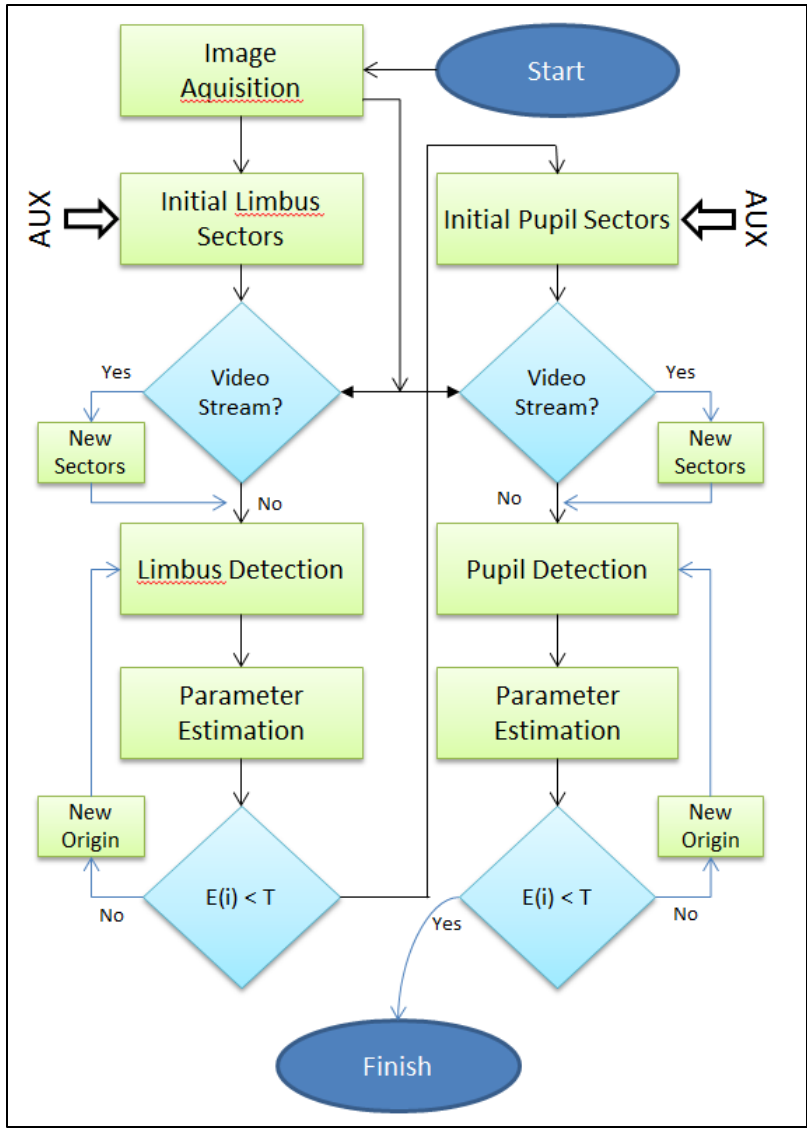


FIGURE 1: FLOWCHART OF THE PROCEDURE USED FOR AUTOMATIC PUPILLOMETRY (ISKANDER, 2004)

The literature (cited above) provides mathematical calculations that will need to be evaluated for applicability in this project. Each step in this pupillometry algorithm will need to be analyzed based on parameters (e.g. sampling rate). The overall hardware setup could potentially disallow for certain mathematical operations to be useful. Therefore, this literature review has provided information regarding one pupillometry algorithm; however, in order to optimize the accuracy of the system, the Team will likely draw from various pupillometry algorithms.

2.6 POTENTIAL ARTIFACTS

Measurement artifacts are physical impairments that can interfere with acquiring relevant, accurate data. Artifacts are identified, and then alterations are implemented to reduce the noise, which is introduced by the artifact during measurement. The proposed system shall utilize optical measurements, and therefore artifacts, such as focus, image size, and target location, are introduced. Furthermore, this system is acquiring electrical measurements through a common off-the-shelf Sony charge-coupled device (CCD) camera. Therefore, factors including sampling rate and timing offset must be considered, and design decisions must be made based upon these considerations.

Artifacts, in which design decisions are being made to reduce the amount of impairment introduced, are focused on a variable factor of the system: the subject. The premise of the operation of this device is based upon physiological responses of the subject; however, a physiological phenomenon known as ocular microtremor (OMT) must be considered in order to reduce measurement noise. Additionally, the subject will be free to move (head and/or body, considered a rigid body in three-dimensional space, with six degrees of freedom) within the image space. Design decisions must reflect the fact that the subject can move outside of the image space. Additionally, the subject's face may not always be facing (perpendicular to) the image capture device, which could introduce measurement errors. These attributes are discussed in further detail, below, to provide a background on some of the potential measurement artifacts, which were considered in the design of the device.

OCULAR MICROTREMOR

Ocular microtremor is a high frequency (60-110 Hz), low amplitude (120-2500nm) tremor of the eye. This physiological response is due to constant brain stem activity that is ever-present in humans and is theorized to function to correct displacements in eye position produced by ocular drifts. The variation in frequency (mean = 86 Hz, $\sigma = \pm 6$ Hz) is caused by differences in brain stem activity. For instance, a study conducted by Mercer's Institute for Research on Ageing (St. James's Hospital, Dublin, Ireland) in conjunction with Frenchay Hospital's Department of Neurosurgery (Bristol, UK) that subjects with clinical evidence of brain stem or

cerebral disease or dysfunction displayed a statistically significant lower frequency of ocular microtremor [Bolger, 2000]. The study attributed these findings to impaired brain stem function.

Proper engineering design of sampling rate, signal and image processing, and other data acquisition parameters of a pupillometer system must be implemented to compensate for this physiological response. First, relative to the frequency of OMT, the system must sample at a rate greater than 220 Hz (two times greater than the maximum frequency of the ocular microtremor) per the Nyquist-Shannon Sampling Theorem. Implementing this sampling rate will ensure that these small changes in pupil diameter are acquired during data acquisition. This will provide data for the algorithm development to minimize the error caused by this physiological response.

HEAD/BODY MOVEMENT

In an average measurement setting, the subject has the freedom to move within the image space. Movements, in every dimension, will have an effect on the ability for the algorithm to complete a high-accuracy measurement. Therefore, design decisions must be implemented to ensure that each of these movements can be identified and accounted for. For a subject changing depth in the field of view, a telecentric lens has been incorporated to operate over a working distance in which the image size of the subject will not change based on depth. Additionally, a subject will be able to move laterally and horizontally within the image space; functions have been incorporated into the algorithm to detect the presence of the pupil anywhere in the image space, rather than just in the center. Additionally, error-handling conditions have been implemented to identify when the subject's pupil has been removed from the image space.

III. PROBLEM STATEMENT

Current methods of pupillometry testing use various applications of similar theories; the pupil of a subject is viewed and diameter is recorded. Many systems use active illumination to illuminate the pupil, which is then captured by an imaging device at a small distance. Because of this general design, current devices are limited in their applications, and there exists a gap in research concerning the effects of a varying of the illumination source and increased subject distance. A method for obtaining measurements of pupil diameter, which does not interfere with the behavioral tasking or physiological conditions of the subject, is essential for the development and innovation of further applications of pupillometry.

PROJECT GOAL

The goal of this project is to develop, design, fabricate and test a functional prototype which is able to monitor and record changes in pupil diameter from a distance of two (2) meters. The prototype shall include software means of detecting and avoiding measurement errors caused by eyeglasses, varying iris color, varying ambient lighting conditions, corneal reflections, and eye blinking. The system shall be accurate within 0.1 mm, in order to collect data that will be relevant in potential applications.

IV. DESIGN METHODOLOGY

The project team performed the design process according to Clive L. Dym and Patrick Little [Dym, 2009]. The steps taken to complete the design process will now be described in detail. Throughout this process, special considerations were paid to the interests of the client and stakeholders.

4.1 CLIENT STATEMENT AND DESIGN GOALS

The initial statement of the project provided to the design team from the client stated: “Design, construct and test a functional prototype, which has the means for obtaining high-quality ocular measurements including, but not limited to sizes of irises and changing pupil diameter of non-stationary people with remote, standoff sensors.”

A list of objectives for the design of the device was developed through continuous interaction with the client and stakeholders of the project. This was completed through multiple interviews and questionnaires, in addition to a literature review conducted by the project team pertinent to current pupillometry technology. The following are objectives for the design of the device:

- Is lightweight.
- Is portable.
- Is stand-alone.
- Is safe to all direct and indirect users.
- Is accurate.
- Is precise.
- Is reliable.
- Is useful.
- Is inexpensive.
- Is durable.
- Is designed for manufacturability
- Is marketable

1. Stand-alone (lightweight & portable): For ease of integration of the device into the client’s system, the final design must be lightweight and portable. This will decrease the cost to the client when purchasing a pan/tilt unit for the device to be housed in. Additionally, portability will increase the ease of testing for verification and validation of the system.

2. *Useful (accurate & precise)*: The client expressed a high level of importance regarding the accuracy, precision, and repeatability of measurements made by the proposed device (identified through the use of a pairwise comparison chart shown in Table 2, below). These objectives will be optimized through hardware design, in addition to meticulous testing and algorithm development and alteration.

3. *Marketable (reliable, inexpensive & designed for manufacturability)*: The final design must optimize usefulness during operation, while maximizing reliability and minimizing development cost. Reliability will be achieved through the use of high-quality hardware components. To design the device to be inexpensive, the Team will utilize common off-the-shelf components, which also contributes to accomplishing the objective of designing for manufacturability. Figure 2, below, displays an objectives tree for the design of the device, which was created by placing the objectives (specified above) into a hierarchy.

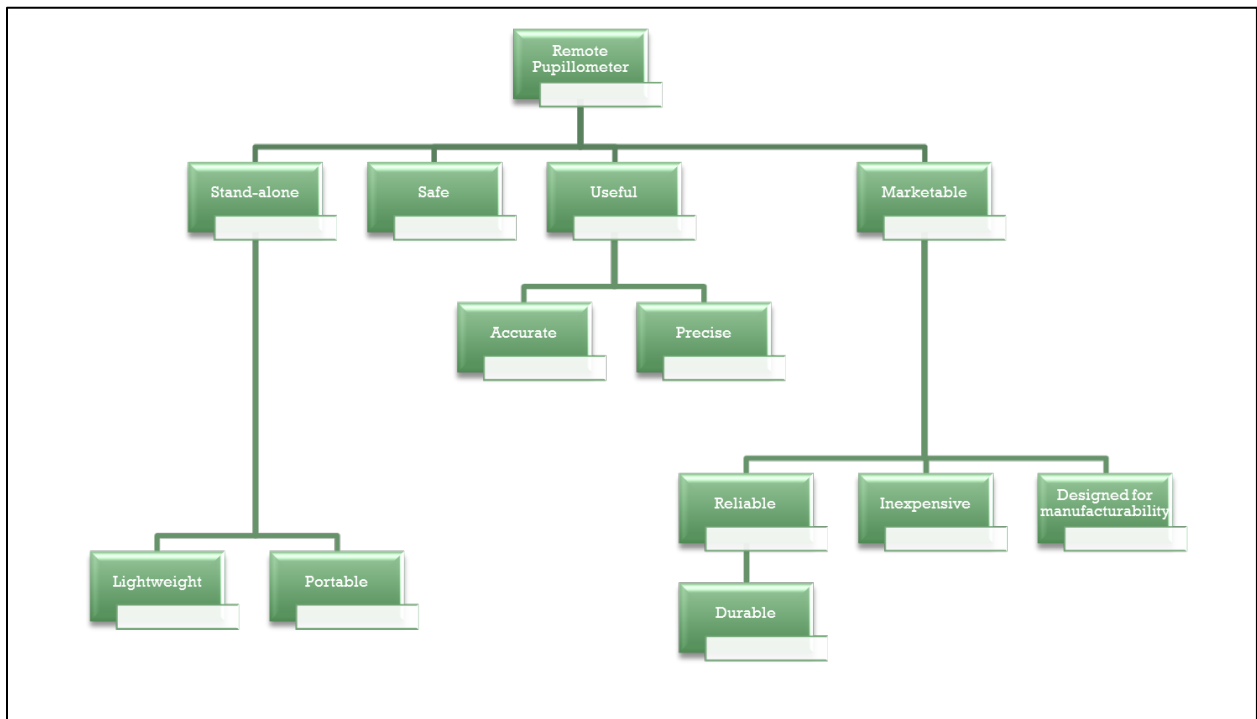


FIGURE 2: OBJECTIVES TREE

During the design of the device, the design team considered the primary functions that system needed to complete in order to meet the needs and expectations of the client. The following list displays the functions that the device must accomplish:

- Will locate the pupil
- Will illuminate the pupil
- Will measure pupil diameter
- Will operate remotely
- Will capture measurements
- Will analyze measurements
- Will display data/results

The client also identified several constraints for the design. These requirements were pertinent to the project schedule and budget, in addition to size and weight constraints due to the project plan to integrate the designed device into a larger system. The following are the design constraints for the project, and descriptions for each are provided thereafter:

- Must be completed by April 1st, 2012
- Must include a variable light-intensity source
- Must be capable of performing measurements with minimal active illumination
- Must be completed within budget of \$10,000
- Must be smaller than 1 ft³
- Must weigh less than 10 lbs.
- Must integrate with Draper Laboratory pan/tilt stage

1. Project deadline

The project must be completed by April 1st 2012 because the schedule for the larger system being developed by the client is dependent on the completion of this system.

2. Variable bright-pupil illumination

The client stated that the design must have a variable light-intensity illumination source. The project Team will work to characterize the accuracy of the system as a function of the light-intensity of the illumination source. Furthermore, the Team will analyze the accuracy of the system when no integrated light source is used to illuminate the pupil.

3. Project budget

The budget threshold set by the client for this project is \$10,000. Additionally, all items purchased by the Team will be delivered to the client at the completion of the project regardless of whether the item was used in the final deliverable.

4. Factors dictating device integration with Draper Laboratory pan/tilt unit

An objective identified by the project team is that the device must be lightweight. Furthermore, the device must be smaller than 1 ft³ in order for the device to be easily integrated into the larger system being developed by the client. Due to this concern, the device must also weigh less than 10 pounds.

4.2 EXPERIMENTAL DESIGN

Before investing time and resources to developing and fabricating design alternatives, the design team first used various methods to quantify the information, objectives, and requirements set by the client. The following section describes these methods, the resulting information, and the rationale used to move forward to in the design process.

The first method used to rank the importance of the high-level objectives set by the design team and the client was the pairwise comparison chart. This ranking has been evaluated by the client for consistency, and confirms the assumptions made by the Team. These assumptions were developed through the use of various design tools based on communication with the client. Additionally, although safety for all direct and indirect users was noted as an objective, it was not considered for comparison among other design objectives, because it is also a design constraint required by the client. The pairwise comparison chart for the overall design objectives is shown in Table 1, below.

TABLE 1: PAIRWISE COMPARISON CHART: OVERALL DESIGN OBJECTIVES

	Useful	Stand-alone	Marketable	Score
Useful	X	1	1	2
Stand-alone	0	X	1	1
Marketable	0	0	X	0

Following the ranking of the high level objectives, it is important to rank the sub-objectives within each high level objective. Table 2, below, shows the analysis of the sub-objectives for the high level object of the device being useful. It is important to note, that although the client desires that the device operate at a distance from the subject, it is of higher importance for the device to be accurate and precise.

TABLE 2: PAIRWISE COMPARISON CHART: SUB-OBJECTIVE (USEFUL)

	Accurate	Precise	Operate Remotely	Score
Accurate	X	1	1	2
Precise	0	X	1	1
Operates Remotely	0	0	X	0

Table 3, below, shows the analysis of the sub-objectives for the high level objective of the device being stand-alone. It was determined that the Team will place a higher design priority to creating a final product that is lightweight for integration within the client’s current system. Although it is of higher importance to design the product to be lightweight, the project team will still optimize the design to be portable, as well.

TABLE 3: PAIRWISE COMPARISON CHART: SUB-OBJECTIVE (STAND-ALONE)

	Lightweight	Portable	Score
Lightweight	X	1	1
Portable	0	X	0

Table 4, below, displays the analysis of the sub-objectives for the high level objective for the device being marketable. Through this analysis and review by the client, the Team determined that is of highest importance for the device to be reliable. Therefore, the device must operate with minimum maintenance and function properly once delivered to the client. Additionally, it was determined that the Team must design the device to be inexpensive. The

team plans on accomplishing this by using common off-the-shelf hardware, which also aids in accomplishing the sub-objective of the device being designed for manufacturability.

TABLE 4: PAIRWISE COMPARISON CHART: SUB-OBJECTIVE (MARKETABLE)

	Reliable	Inexpensive	Designed for Manufacturability	Score
Reliable	X	1	1	2
Inexpensive	0	X	1	1
Designed for Manufacturability	0	0	X	0

After assessing the initial client statement, conducting interviews with stakeholders and reviewing client communication, the team revised the client statement to the following:

“Research, design, construct and test a functional and portable brassboard prototype for remote pupillometry testing with remote, common-off-the-shelf (COTS) components. The image-capturing portion of the device will utilize a black and white camera. Designs are subject to the specifications and needs provided by the Client, and the primary components of the design include a variable-intensity NIR illumination light source, a remote camera and input processing unit to assess the level of fatigue in a subject and must be safe to all direct and indirect users.”

4.3 CONCEPTUAL DESIGN

Hardware components for the proposed system must be analyzed for applicability of integration. Each main component is outlined in detail in the following section, which summarizes the considerations that will drive the final hardware design. The reasoning of the overall approach is broken down into each component and how it fits the overall project design.

IMAGE CAPTURE DEVICE - CAMERA

To capture the refracted image of the pupil, a black-and-white video camera will be used. Using a camera will be the most effective method of accurately capturing pupil diameter and analyzing in real-time. Other methods were assessed and found to be ruled out due to acquisition rate, cost, accuracy and repeatability.

The camera will provide a method to capture images of the subject, in order to provide raw data for the software algorithm to perform analysis. The camera will be used to perform the function of capturing measurements specified for the proposed device. It will also provide the data necessary to locate the pupil, and furthermore, measure the diameter of the pupil.

Because the camera will capture original data for analysis, it is critical that a camera with proper specifications (e.g. resolution) be chosen for the system. Additionally, it is imperative to consider how the camera will be integrated into the system and function with other components. The camera must possess a lens mount that is compatible with the lens (through direct connection or an available adapter) for proper component integration. Furthermore, if an analog camera is chosen, the output of the camera is required to be a cable type that is appropriate for the proposed frame grabber card.

In consideration of the design objectives and constraints, it is essential to characterize how the specifications and performance of the camera component of the system will affect such goals. The camera must not cause the system to fail to meet the dimensional size and weight constraints specified by the Client. In addition, the camera must be chosen with close consideration of the overall budget for the project.

Various types of cameras are available for this design that do not impede on completion of the considerations listed above. Cameras can operate analog or digitally. An advantage of choosing a digital camera would eliminate the need for a frame grabber card (analog-to digital conversion); however, then another method for importing the data into a computer-based system would need to be explored and developed. To minimize cost, the camera chosen will be black-and-white, as color is unnecessary for this application. Additionally, the image pickup device (e.g. complimentary metal-oxide-semiconductor (CMOS) or charged-couple device (CCD) sensors), sensitivity and minimum illuminance are other factors that will be considered when choosing a camera for the system.

OPTICAL INPUT CONTROL - LENSES

To alter and control the image received by the camera, various lenses or combinations of lenses will be used to change the image input and compensate for distance, angle and movement. The lens(es) will provide a method to control the image space being captured by secluding the space in the sight of the camera. This will aid in completing the functions of locating the pupil, capturing measurements and measuring pupil diameter. Although there are no functions that are specific to this component, correct lens choice will be vital to the overall performance of the system.

Several specifications will need to be considered to choose an appropriate lens for the system, which include focal length, aperture and zoom. These factors will determine how the raw image captured by the camera appears, which can drastically impact the design of the software algorithm for analysis.

The lens will be responsible for analyzing or adapting to the user being at different distances from the camera. Otherwise, as the subject moves farther away, the image of the pupil will appear to be smaller. Although the subject will be at a known distance and known location from the camera system, it will be effective to design this system to perform at varying distances to increase the capability of the system for the client, as so long as this decision does not obstruct the Team from adhering to all design constraints. If the Team chooses to design this component to increase system capability and adaptability, a telecentric lens, in which the size of the captured image does not change as a function of distance from the capturing device, would be appropriate.

LIGHT FILTERING - OPTICS

Additional optics could be integrated into the capturing system in order to improve performance or increase the capability of the device. Optical filters that stop specific wavelengths of light and pass other wavelengths would be an effective method to eliminate pieces of the raw image that are not necessary for analysis. This component will function to aid in capturing measurements. Careful analysis of filter specifications is necessary to determine how the component will function within the system, and how, in terms of physics, the component will improve the overall function of the device.

Furthermore, optical filters can be used to filter the illumination source, thus increasing the safety to the subject. Although the chosen illumination source may emit a specific wavelength (or range of wavelengths), subject safety can potentially be increased by filtering the emitted wavelengths of the illumination source. This will not only decrease the amount of potentially harmful light that is emitted but will also decrease ‘noise’ and potentially provide a cleaner signal for processing.

PUPIL ILLUMINATION SOURCE

For an illumination source, the team reviewed light-emitting diode (LED), halogen and laser sources. Many factors need to be considered when choosing an illumination source for the design, which include repeatability, durability, safety, and emitted wavelength. Emitted wavelength will play a role in the other considerations for the component, thus it was the primary factor for analysis. The human pupil reacts to light stimuli by changing diameter to optimize vision. Therefore, the illumination source should be chosen as to minimize this physiological response (and therefore optimize system accuracy). Significant reduction in pupil size has been observed at an illumination wavelength of 715 nm and iris closure has been identified when illuminating the pupil at 830 nm [Devereux, 1995]. Because, the device will operate remotely and detection of the system should be minimized for marketability and ease of integration with the client’s system, it would be effective to choose an illumination source that operates at a wavelength that is not detectable by the human eye (outside of the visible spectrum). Using this approach, the proposed illumination source should emit wavelengths outside of the range of 390 to 750 nm. Through a literature review of current pupillometry devices, it was identified that current active-illumination devices utilize sources that emit wavelengths between 830 and 900 nm.

With safety for all direct and indirect users being a constraint for the design, it is imperative to choose an illumination source that adheres to this consideration. Because lasers and halogen illumination sources pose an increased risk to the safety of the subject (dependent on beam angle, power density and other factors), an LED could be an appropriate design choice for the illumination source.

The repeatability and durability of the illumination source must also be considered. These factors will be optimized through review of product performance and specifications. It may also prove effective, if the project schedule allows, for the Team to characterize the performance of the device using various illumination sources. This analysis would not only provide additional data and conclusions to the client, but also aid in improving the overall performance of the system.

CABLING

Communication is a necessary component of the device functionality. As each component requires different cabling, each cable was carefully chosen for proper compatibility between the components.

The Sony XC-EI50 uses a 12-pin multi-connector. After looking at a variety of options available, the Hitachi 45601-C9 was chosen. This cable is compatible with Sony and Hitachi 12 pin cameras and integrates the required power supply, requiring fewer components. The video output is provided via a BNC connector.

The ALTA PCE-AN1 requires a custom cable for use with BNC connectors, which was ordered from the manufacturer due to resource allocation. This cable is designed for use with all Alta frame grabbers. The wiring diagram of this custom cable may be found in Appendix A: Product Datasheets.

V. THE REMOTE PUPILLOMETER – OVERVIEW

The following section provides an overview of the Remote Pupillometer system. The full system block diagram is introduced with a description of the main functional components. The theoretical behavior of the system is then described to provide information regarding the performance that the device was designed to achieve.

5.1 BLOCK DIAGRAM OVERVIEW

The Remote Pupillometer device consists of four major functional blocks: Image Acquisition, Illumination Circuit, Data Acquisition, and Computer Processing. The block diagram can be seen in Figure 3.

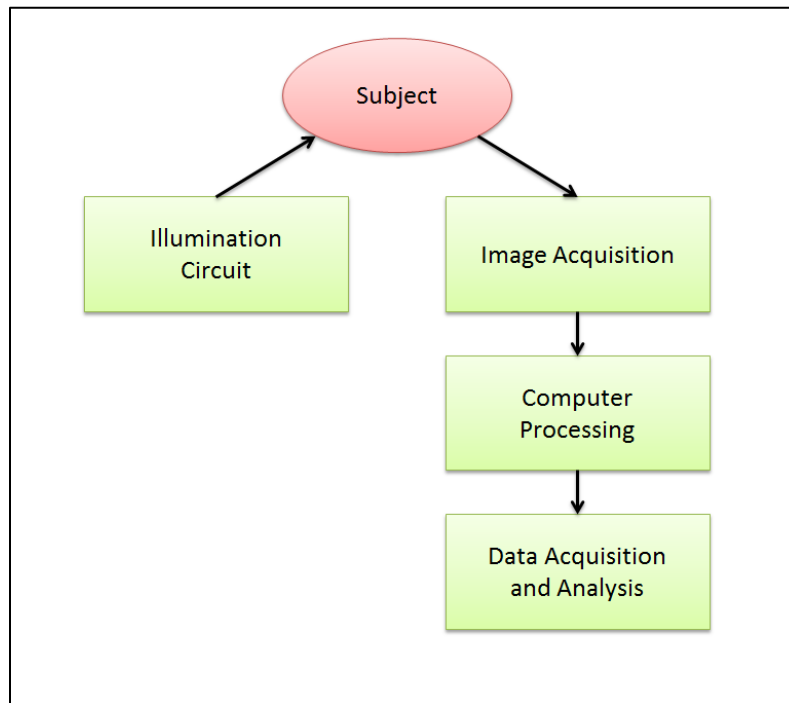


FIGURE 3: HIGH-LEVEL SYSTEM BLOCK DIAGRAM

IMAGE ACQUISITION

The design of the image acquisition hardware and conceptual operation was completed through much iteration. The Sony XC-EI50 analog camera was chosen based on its size, price, and applicability for this project; however, the illumination source (NIR emitter) design required extensive designing, testing, and validation. After identifying the bright pupil effect as a phenomenon that could be utilized to isolate the pupil in the image space, further research was needed to determine the appropriate component. Specifications that were considered while choosing the NIR emitter included wavelength, power output, operating current, and beam angle. Through this design process, the team was able to fabricate an illumination source that functioned appropriately for this stage of development, which is discussed in detail in this section; however, as development continues, further testing will be required to identify the NIR emitter that is most appropriate for this application.

ILLUMINATION CIRCUIT

The illumination source used in the system was developed to create pseudo-coaxial NIR illumination to the subject. This was completed by assembling the emitters in an equidistant circular pattern on rings that were attached to a lens-adaptable hood. A photograph of the illumination source is provided, below, in Figure 4.



FIGURE 4: ILLUMINATION SOURCE

The illumination source was powered with 13 V using a Hameg Programmable Power Supply (HM7044). An electrical schematic of the outer ring of the illumination source is provided in Figure 5, below. The inner ring of the illumination source is identical, except it uses 21 NIR emitters, rather than 24.

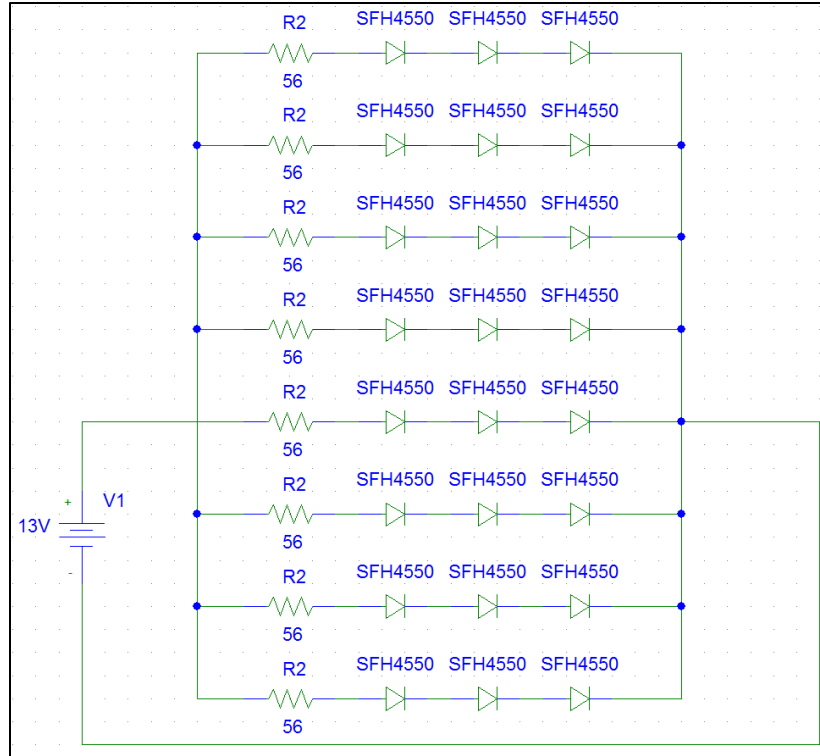


FIGURE 5: OUTER RING SCHEMATIC

DATA ACQUISITION

In order to make the data available for computer analysis, a hardware component was needed to convert the analog data (output from the camera) to digital data. Therefore, an analog-to-digital converter (ADC) was required to be integrated into the system. In the field of image processing, this device is known as a frame grabber, because it is acquiring an array, or frame, of data rather than a single data point.

A major requirement during the design of the system was that the data be easily imported into MATLAB for processing. Therefore, a frame grabber that was supported by (and compatible with) MATLAB was chosen. The BitFlow Alta-AN1 frame grabber card was chosen and integrated into the system.

COMPUTER PROCESSING

The computer software algorithm for monitoring the change in the pupillary diameter was designed using MATLAB version R2011b software (Mathworks, Natick, MA). This particular software package was selected based on the compatibility with the chosen analog framegrabber card, in addition to the extensive built-in image processing functions, known as the Image Processing Toolbox. Additionally, the software is licensed through Worcester Polytechnic Institute, which made for a cost-effective choice, rather than purchasing an alternative software package.

The software is still currently in the form of a functional prototype in order for the client to complete further testing and data analysis. In this stage of development, the program is set to monitor the subject for a specific amount of time (e.g. 30 seconds). First, the program initializes by clearing the workspace then configures the video source for acquisition. Once a new frame is available for processing, the function passes the frame data to `pupilProcess.m`, a function developed to calculate pupil diameter for this application. Following successful processing, the function displays the percentage change in pupil diameter from the previous frame in the MATLAB workspace. If the function determines that the frame was processed incorrectly, however, it will ignore the frame and move to the next available frame. The data of calculated percentage change values are stored in an array, which is output by the function. The flow of the main function `pupillometry.m` is depicted, below, in Figure 6.

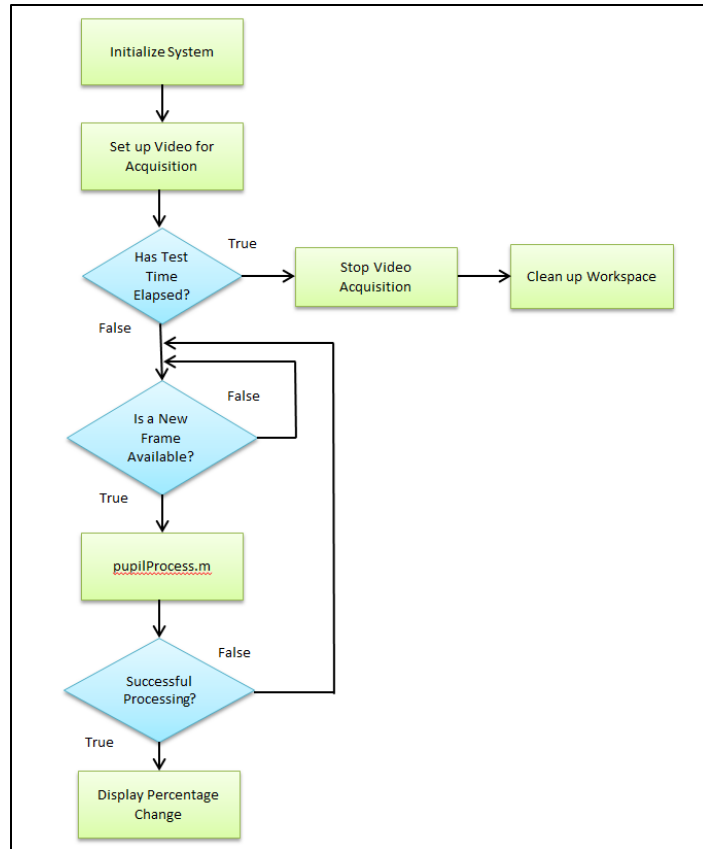


FIGURE 6: HIGH-LEVEL SOFTWARE FLOW DIAGRAM OF PUPILLOMETRY.M

The majority of the image processing and data analysis is completed within the MATLAB function *pupilProcess.m*. The algorithm was designed to be adaptive, and utilizes feedback from the previous frame to set algorithm parameters. The design choice to utilize feedback from the previous frame was implemented, because the high sampling rate (in comparison to the maximum frequency of pupil diameter change) implies that no major changes in the image space will occur between samples. The basic structure of the function *pupilProcess.m* is depicted in Figure 7, below. A detailed explanation of each block is provided, below, as well.

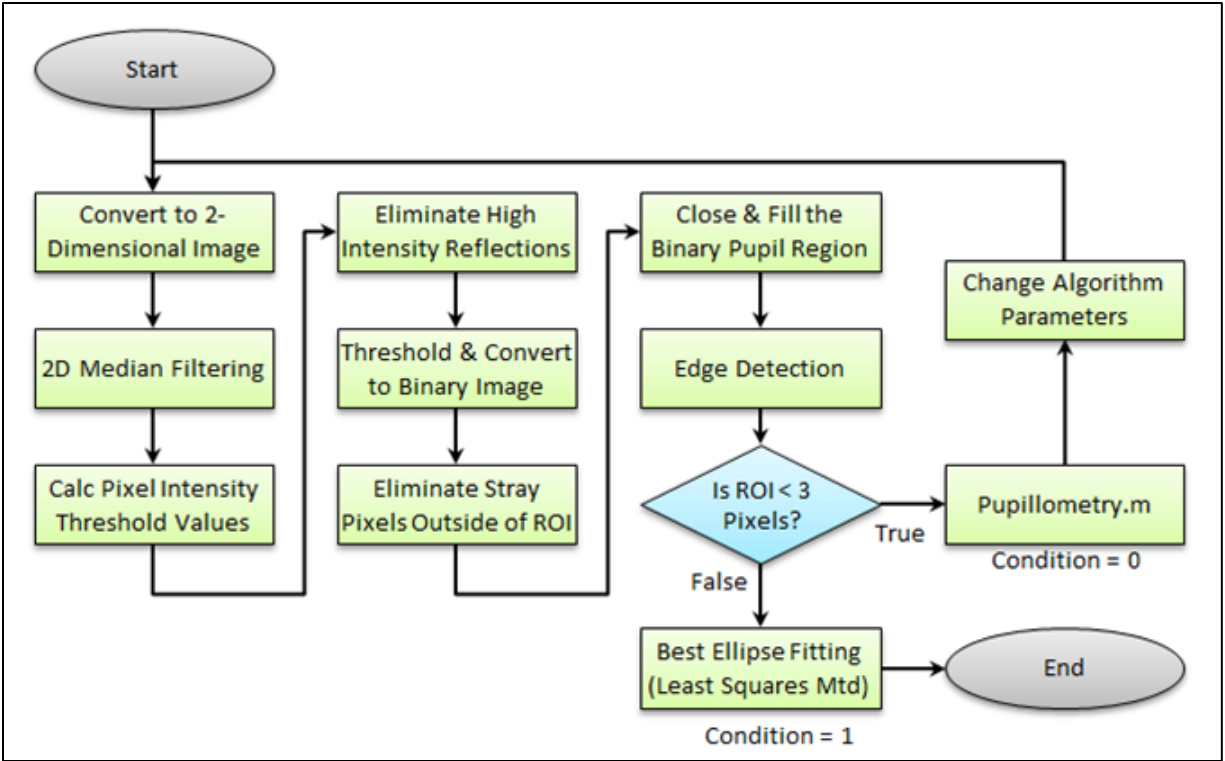


FIGURE 7: SOFTWARE FLOW DIAGRAM FOR PUPILPROCESS.M

The image that is passed into the function *pupilProcess.m* from *Pupillometry.m* must be manipulated into a form that can be processed by the function. First, the function must convert the input image to a 2-dimensional image. This system utilizes a gray scale analog camera, so this operation is not necessary; however, this allows for the integration of a color image acquisition device in the future. Figure 8, below, depicts a sample of the original image that is input into the pupillometry algorithm for processing. Next, two-dimensional median filtering is performed to smooth the image and remove any noise caused by movement of the subject or changes in ambient lighting conditions.



FIGURE 8: ORIGINAL IMAGE INPUT TO PUPILLOMETRY.M FOR PROCESSING

Conditions of the environment in which the measurements are being conducted (e.g. reflective material within the image space) can decrease algorithm accuracy and performance. After confirming this information experimentally, it was necessary to design an algorithm to adapt to changes in these conditions in order to isolate the pupil correctly for measurement.

Given an illumination source that outputs constant power over time, it is possible to utilize image intensity analysis to determine upper and lower threshold values for conversion to a binary image. This process is designed by creating a histogram that has a bin for each pixel intensity value (0-255). Due to the optical bandpass filter, most pixels will be darker, and therefore, closer to 0 on the image intensity scale. The algorithm developed searches each bin of the histogram beginning at 30 until a bin contains less than 40 pixels of that intensity. The value of 40 was chosen experimentally, and this implies that a proper lower threshold value has been detected. Next, the algorithm continues to increase the bin index searching for a bin, which contains an amount of pixels with the same intensity that is greater than 100. This detection implies that a reflection has been detected at this intensity, and all pixels with intensity greater than this value should be eliminated from the image prior to further processing. A histogram of pixel intensity of a sample image with no other high intensity reflections is shown in Figure 9.

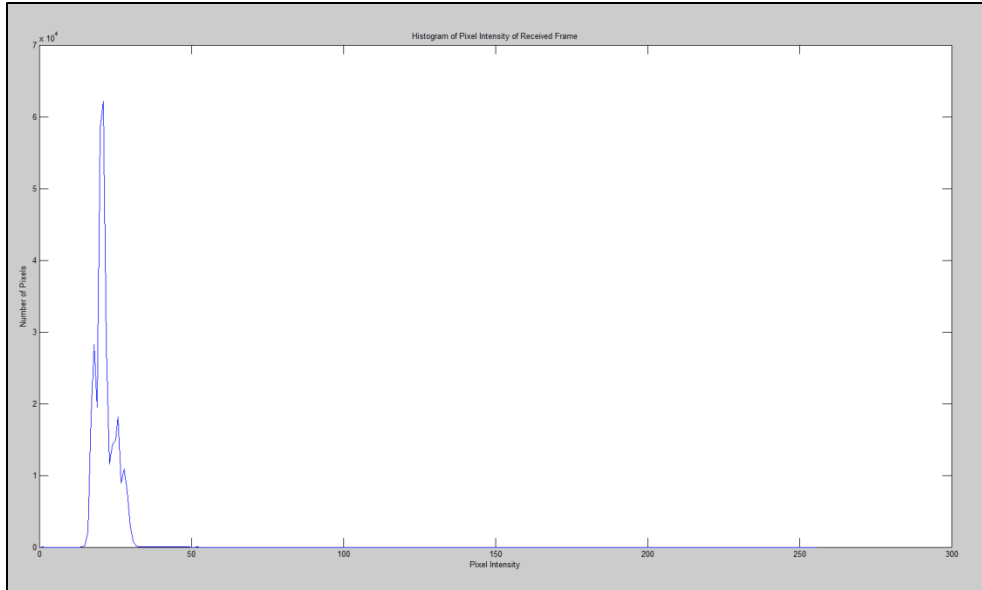


FIGURE 9: HISTOGRAM OF PIXEL INTENSITY OF A SAMPLE IMAGE WITH NO OTHER REFLECTIONS

The cutoff values calculated in the previous step of the algorithm are used to remove potential artifacts that arise during image acquisition. Using the high threshold value, the function eliminates high intensity reflections, which are outside of the normal experimentally determined intensity range of pupil retroreflection. Additionally, the function uses the low threshold value to convert the image to a binary scale of black and white pixels. Converting to this format, following the initial preprocessing steps, allows for much more efficient and accurate computation and analysis. Additionally, during the thresholding process, the identified region of interest (i.e. pupillary region) is closed and filled. Figure 10 depicts (a) the original image, and exhibits the isolation of the illuminated pupil in (b) the binary image following thresholding.

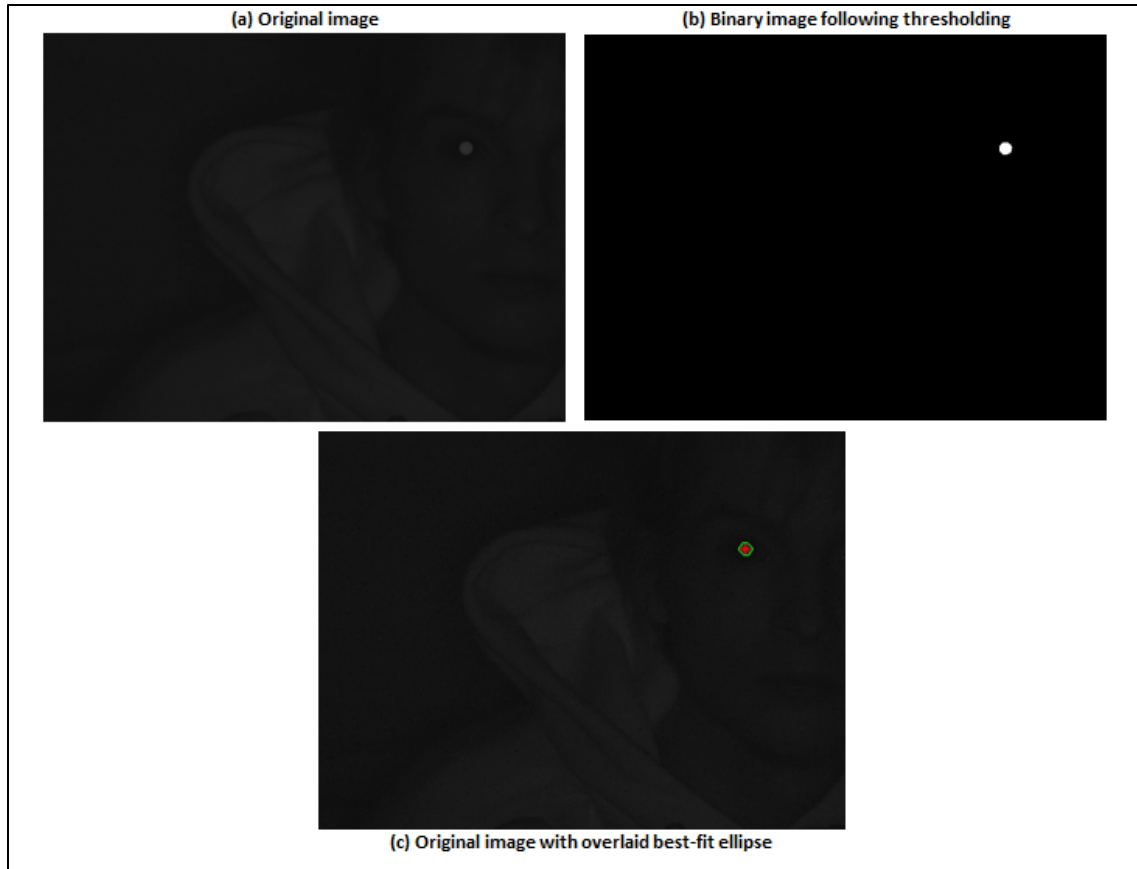


FIGURE 10: COMPARISON OF IMAGES BETWEEN PUPILLOMETRY ALGORITHM PROCESSES

Once the pupil is isolated, edge detection is performed to identify the boundary coordinates between the 0 valued (black) and 1 valued (white) image intensity values. The process of edge detection identifies any coordinate, which is not surrounded by only pixels of the same intensity as the pixel of interest. These coordinates are particularly important, because the array of points is input into best-ellipse fitting (least squares method), which will determine the radius of the region of interest, in addition to compensating and correcting for scenarios in which the pupil is partially blocked by an eyelid, eyelashes, or eyeglasses. The resulting ellipse in comparison to the original image obtained for analysis is shown in Figure 10(c).

VI. RESULTS & DISCUSSION

A considerable amount of data was collected in order to characterize the behavior of the system, in addition to providing initial results regarding system accuracy. The behavior of the system was examined by collecting data relevant to sampling rate and noise floor. Data collected that is relevant to system accuracy included error rate and calculated percentage change versus time. Data regarding system accuracy was collected using a human subject with various acquisition conditions including acquisition with and without background reflections and measurement with and without eyeglass reflection. The data collection process and results will now be discussed in further detail.

NOISE FLOOR

During software testing, it was necessary to determine the maximum amount of error that the system output given a constant input. With data regarding the noise floor of the system, much more informed conclusions can be drawn regarding the operation of the device. The test was designed to monitor the reflection of the active illumination source off a corner cube, therefore, creating a constant source of reflection that closely resembles the retroreflection of a pupil. Several iterations of this test were conducted to obtain statistically significant results. Additionally, various lighting conditions were tested to examine if changes in lighting of the operating environment has any effect on the accuracy of the system.

The test allowed the project team to draw numerous conclusions. First, due to the insignificant change in the maximum noise level between a lighted environment and a dark environment, it was concluded that lighting conditions will not affect the operation of the device. This conclusion is consistent with predictions based upon the design choice to utilize the 850nm bandpass filter to eliminate any noise or impairments caused by ambient light.

The maximum noise level for the system was determined to be 0.5%. Data collected in one-minute durations (data was also collected in five-minute test durations) was analyzed and statistics are displayed in Table 5, below.

TABLE 5: NOISE LEVEL TESTING DATA (ONE-MINUTE DURATION)

	200cm	250cm	300cm
Mean	-0.003	-0.002	-0.014
Std. Dev.	0.902	1.079	1.850
Min	-2.536	-3.204	-6.000
Max	2.769	3.001	5.651

The data provided in Table 5, above, was analyzed by taking the absolute value of the array of percentage change. The percentage change values were centered at 0, which indicates that there is likely no offset value. A plot of the percentage change over a duration of one minute is depicted in Figure 11.

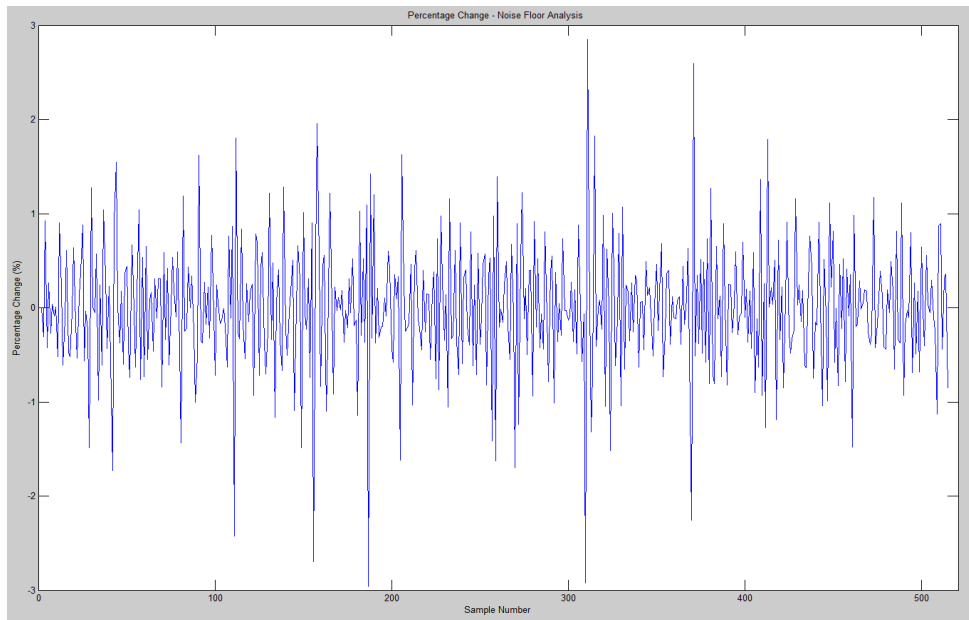


FIGURE 11: PLOT OF NOISE LEVEL TESTING DATA (1-MINUTE DURATION)

The determined noise floor should allow the system (in its current state of development) cannot operate within the desired accuracy specification. During further development, this

characteristic could be improved by integrating a camera with higher resolution. Additionally, the noise level could be decreased by optimizing and further improving the adaptive thresholding algorithm. Recommendations for further development of the system are provided on page 39.

FRAME RATE

As seen in previous research, two types of oscillations exist: slow waves lasting 4-40 seconds and fast waves ranging from 0.5 to 1 second. [Lowenstein, 1963] In order to best acquire data and assess a subject, the system needs to operate at a frame rate at least 10 times faster than the fastest movement, or a rate of 20 Hz. The device as currently designed operates at a rate of 8.75 Hz. Therefore, the system is currently able to process 8.8 image frames per second. The frame rate could be greatly improved through MATLAB code optimization. To allow for smoother data analysis, the system optimally would operate much faster. This would be accomplished with an integrated system, but for preliminary testing purposes, this rate achieves the intended results.

PUPILLOMETRY ALGORITHM ERROR RATE

Various image acquisition scenarios were examined to characterize the efficacy and robustness of the developed algorithm. A common element that was noticed during initial testing was the presence of reflection off of objects in the background of the subject. A study was conducted to determine the effect of this reflection on algorithm performance by creating a constant background reflection in the image using a corner cube. The data collected is shown, below, in Table 6. The algorithm is able to still operate efficiently and with few errors, and there is not a significant increase in errors between the two conditions. Additionally, the errors could be caused by the subject blinking, which is a measurement case that the algorithm cannot handle in this stage of development.

TABLE 6: ALGORITHM ERROR RATE WITH AND WITHOUT REFLECTIONS

Test Number	Errors without Reflections	Errors with Reflections
1	0	3
2	2	1
3	0	0
4	1	1
5	0	1

In addition to the presence background reflections, the developed algorithm was also designed to correctly process frames when the subject is wearing eyeglasses. This portion of the algorithm has proven to be successful during initial testing; however, it has also failed in some instances. Because the intensity of the retroreflection of the pupil is much less than the reflections off of objects (e.g. eyeglasses) within the image space, the algorithm is able to analyze that intensity to locate the pupil. However, because the algorithm operates adaptively as it processes each frame, the feedback provided to the algorithm can cause the pupil retroreflection to be eliminated from the image. Figure 12, shown below, displays the output image of the pupillometry algorithm when analyzing a subject wearing eyeglasses. In this instance, the algorithm processed the frame correctly; however, during the processing of some frames, the algorithm will isolate one of the eyeglass reflections rather than the pupil retroreflection.



FIGURE 12: OUTPUT IMAGE FOLLOWING PROCESSING WITH EYEGGLASS IMPAIRMENTS

Further algorithm development and testing will resolve this intermittent deviation from the region of interest. Additionally, as noted in Recommendations, the integration of a more appropriate illumination source for this application could initiate great improvement in this area of image processing.

FATIGUE ANALYSIS

Although the detection of fatigue in a subject was a motivating factor for this project, at this stage in development, the system is not accurate enough to complete this type of analysis. Fatigue analysis is an application of pupillometry, and the development of the capabilities of the system (e.g. remote measurement) constitutes as extensive progress in the field. The purpose of the project, given by the client, was to develop a system that was capable of obtaining high-accuracy ocular measurements. Currently, the system is able to conduct measurements, and recommendations for the improvement of the accuracy and precision of the system have been provided.

VII. RECOMMENDATIONS

Future work for this device could take various forms. At this stage in development, there are various factors that need to be improved and additional implementations that need to take form in order for the system to function properly. Specific conditions exist that are outside of the scope of this project, and potential solutions were realized. This portion of the work aims to provide the client with information so that the development of the system can be continued and eventually finalized.

One recommendation for future work is to improve the sampling rate of the system. During the testing and verification phase, this was identified as a factor, which could hinder the performance of the device. In MATLAB, a funneling effect can occur, in which the software is unable to process and handle the image frames at a rate that is as fast as the frames are being acquired. Additionally, the system can only acquire frames of the live video feed as frequently as the software can complete processing. Therefore, MATLAB code optimization, specifically, the removal of processing and analysis by looping, may decrease the processing time of each frame. The MATLAB code associated with eliminating unwanted reflections is called recursively, which substantially increases the time necessary for image processing. Profiles regarding the MATLAB code can be found in Appendix D: MATLAB Code Profiles. Because this application requires a high frame rate, it is recommended that the system (currently operating on a personal computer), be transferred to an embedded system. This could be complete through the use of an application-specific integrated circuit (ASIC) or a field-programmable gate array (FPGA).

Another issue related to the system at the current stage in development is that the noise floor is relatively large, which could restrict the acquisition of high-quality measurements. As previously stated, at times, noise levels of up to 8.4% were incurred during testing. There are multiple steps that must be taken to decrease the noise level. First, the MATLAB code must be rigorously tested to determine where inaccuracies are occurring. Specific to hardware, the relative size of the pupil within the image space must be increased significantly to improve resolution. By integrating a camera with increased resolution, the amount of pixels that contain the pupil will be increased, thus reducing the amount of noise incurred. It may also be effective to integrate a system used to track the pupil within the image space. Once the pupil has been

located, the robust system can automatically zoom and focus on the pupil, which will allow for extremely high-accuracy measurements to be obtained.

During testing, it was determined that the illumination source power and beam-spread was not optimal for pupil retroreflection. By examining the bright pupil effect and conducting further testing, alternative near-infrared LEDs could be identified for use in the system in order to make it easier to distinguish the pupil within the image space. By increasing the power output the illumination source and choosing LEDs with a beam spread of no greater than 10 degrees, the pixel intensity of the retroreflected pupil in this image will be greater. This improvement could also aid in increasing the accuracy and frame rate of the system by allowing for less computationally expensive image processing.

VIII. CONCLUSION

The team was able to successfully fabricate and test a fully functional videographic pupillometer system that is capable of obtaining measurements of a subject from a remote distance. Although the prototype could not be tested among a large sample size of subjects, initial testing indicates that the system, with further improvements, could be utilized in numerous applications of biometric analysis.

The Videographic Pupillometer System is able to obtain measurements from a distance of greater than two meters, which is a large improvement. Some commercially available pupillometer systems require the subject to be in close proximity (e.g. 20 cm) from the device in order to complete measurements. By creating a system that can operate remotely from a subject, the system can obtain measurements without interfering with the behavioral tasking of the subject. As previously stated, at this stage of development, the system requires improvements in accuracy and precision, in addition to increased robustness of the algorithms. However, the team has provided a functional prototype, which displays the conceptual operation of the system. Further development testing will provide insight regarding the improvement of these factors.

The system is able to obtain measurements, and provide data through a graphical interface. The interface displays the obtained image, in addition to the ellipse that was calculated as representing the pupil. Additionally, the system is capable of handling various measurement impairments, such as background reflections, the presence of eyeglasses and eyeglass reflections, and various lighting conditions.

IX. REFERENCES

- Bolger, C., Bojanic, S., Sheahan, N., Malone, J., Hutchinson, M., & Coakley, D. (2000). Ocular microtremor (OMT): a new neurophysiological approach to multiple sclerosis. *Journal of Neurology, Neurosurgery and Psychiatry*, 639-642.
- Cassin, B., & Soloman, S. (1990). *The Dictionary of Eye Terminology*. Gainesville, FL: Triad Publishing Company.
- Dym, C. L., & Little, P. (2009). *Engineering Design: A Project Based Introduction, 3rd Edition*. Hoboken, New Jersey, United States: Wiley.
- Fried, R. (1980). *Pupillometry: The Psychology of the Pupillary Response*. Taylor & Francis.
- Geeraets, W. J., & Berry, E. R. (1968). Ocular Spectral Characteristics as related to hazards from lasers and other light sources. *American Journal of Ophthalmology*, 15-20.
- Iskander, D. R., Collins, M. J., & Trunk, M. (2004). Automatic Pupillometry from Digital Images. *IEEE Transactions on Biomedical Engineering*, 51(9), 1620-1622.
- Laeng, B., Sirois, S., & Gredebäck, G. (2012, January). Pupillometry: A Window to the Preconscious? *Perspectives on Psychological Science*, 7(1), 18-27.
- Lowenstein, O., Feinberg, R., & Loewenfeld, I. E. (1963, April). Pupillary movements during acute and chronic fatigue. *Investigative Ophthalmology*, 138-157.
- Mulvey, F., Villanueva, A., Sliney, D., Lange, R., Cotmore, S., & Donegan, M. (2008). Exploration of Safety Issues in Eyetracking. *Communication by Gaze Interaction (COGAIN)*, Deliverable 5.4.
- Osman, E. A., & Al-Saleh, A. A. (2010). Immediate changes in pupil size following Laser in situ keratomileusis (LASIK): Pupillometry study. *Saudi Journal of Ophthalmology*, 139-141.
- PMI, I. (n.d.). *PMI Inc. - FIT 2000 Fitness for Duty Impairment Screener*. Retrieved December 12, 2011, from PMI Incorporated: <http://www.pmifit.com/>
- Ricci, J. A., Chee, E., Lorandeanu, A. L., & Berger, J. (2007). Fatigue in the US Workforce: Prevalence and Implications for Lost Productive Work Time. *Journal of Occupational and Environmental Medicine*, 49(1), 1-10.
- Richman, J. E., McAndrew, K. G., Decker, D., & Mullaney, S. C. (2004). An evaluation of pupil size standards used by police officers for detecting drug impairment. *Optometry - Journal of the American Optometric Association*, 75(3), 175-182.
- Roorda, A., & Williams, D. R. (1999, February 11). The Arrangement of the Three Cone Classes in the Living Human Eye. *Nature*, 397, 520-522.

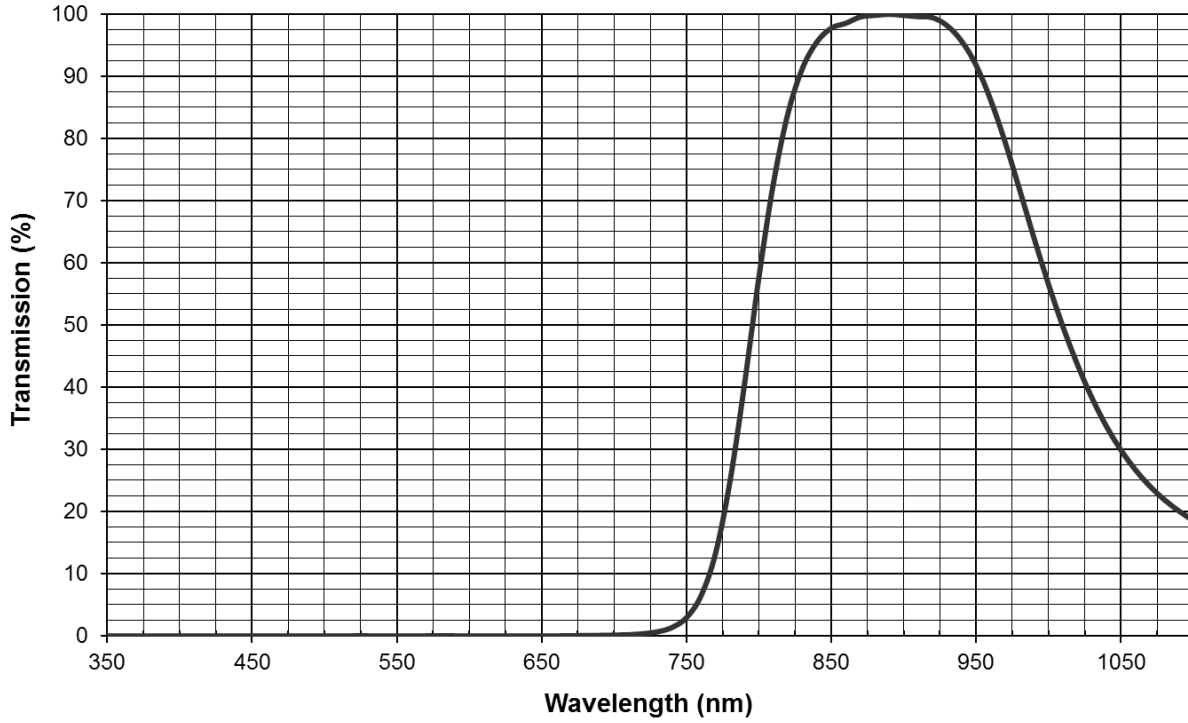
- Siegle, G. J., Steinhauer, S. R., & Thase, M. (2004). Pupillary assessment and computational modeling of the Stroop task in depression. *International Journal of Psychophysiology*, 52, 63-76.
- Smolka, B., Czubin, K., Hardeberg, J. Y., Plataniotis, K. N., Szczepanski, M., & Wojciechowski, K. (2003). Towards automatic redeye effect removal. *Pattern Recognition Letters*, 1767-1785.
- Snyder, J. J. (1975). Paraxial ray analysis of a cat's-eye retroreflector. *Applied Optics*, 1825-1828.
- So, B. S., Jung, Y. H., & Lee, D. W. (2002). Shape design of efficient retroreflective articles. *Journal of Materials Processing Technology*, 632-640.
- Vitabile, S., De Paola, A., & Sorbello, F. (2010, September 15). A Real-Time Non-Intrusive FPGA-Based Drowsiness Detection System. *Journal of Ambient Intelligence and Humanized Computing*, 2(4), 251-262.
- Watanabe, M., & Nayar, S. K. (1997). Telecentric Optics for Focus Analysis. *IEEE Transactions on Pattern Analysis and Machine Intelligence*, 19(12), 1360-1365.
- Whipple, B., Ogden, G., & Komisaruk, B. R. (1992). Physiological correlates of imagery-induced orgasm in women. *Archives of Sexual Behavior*, 21(2), 121-133.

X. APPENDICES

APPENDIX A: PRODUCT DATASHEETS

MIDWEST OPTICAL SYSTEMS INC BP850

BP850 INFRARED BANDPASS



BP850 INFRARED BANDPASS

Data Points

5/23/2006

Wavelength (nm)	Transmission (%)	Wavelength (nm)	Transmission (%)	Wavelength (nm)	Transmission (%)
1100.00	18.52	800.00	57.66	510.00	0.00
1090.00	20.08	790.00	40.40	500.00	0.00
1080.00	21.89	780.00	24.82	490.00	0.00
1070.00	24.05	770.00	13.24	480.00	0.00
1060.00	26.69	760.00	6.43	470.00	0.00
1050.00	29.86	750.00	2.94	460.00	0.00
1040.00	33.67	740.00	1.36	450.00	0.00
1030.00	38.23	730.00	0.66	440.00	0.00
1020.00	43.57	720.00	0.35	430.00	0.00
1010.00	49.66	710.00	0.20	420.00	0.00
1000.00	56.47	700.00	0.12	410.00	0.00
990.00	63.93	690.00	0.08	400.00	0.00
980.00	71.76	680.00	0.05	390.00	0.00
970.00	79.39	670.00	0.03	380.00	0.00
960.00	86.16	660.00	0.00	370.00	0.00
950.00	91.73	650.00	0.00	360.00	0.00
940.00	95.60	650.00	0.00	350.00	0.00
930.00	98.09	640.00	0.00	340.00	0.00
920.00	99.39	630.00	0.00	330.00	0.00
910.00	99.55	620.00	0.00	320.00	0.00
900.00	99.76	610.00	0.00	310.00	0.00
890.00	99.95	600.00	0.00	300.00	0.00
880.00	99.76	590.00	0.00	290.00	0.00
870.00	99.51	580.00	0.00	280.00	0.00
860.00	98.49	570.00	0.00	270.00	0.00
850.00	97.71	560.00	0.00	260.00	0.00
840.00	95.47	550.00	0.00	250.00	0.00
830.00	91.21	540.00	0.00	240.00	0.00
820.00	83.94	530.00	0.00	230.00	0.00
810.00	72.74	520.00	0.00	220.00	0.00

SONY[®]

B/W VIDEO CAMERA

XC-ES50/ES50CE
XC-ES30/ES30CE
XC-EI50/EI50CE
XC-EI30/EI30CE
XC-EU50/EU50CE

Component/OEM**OUTLINE**

The XC-E Series are compact, light-weight one-piece black and white cameras incorporating the latest 1/2 and 1/3 type Interline (IT) CCD which produces new levels of picture detail. With dimensions of 29 x 29 x 32 mm (1³/₁₆ x 1³/₁₆ x 1⁵/₁₆ inches), these cameras can easily be installed in places where installation was previously difficult for other larger cameras.

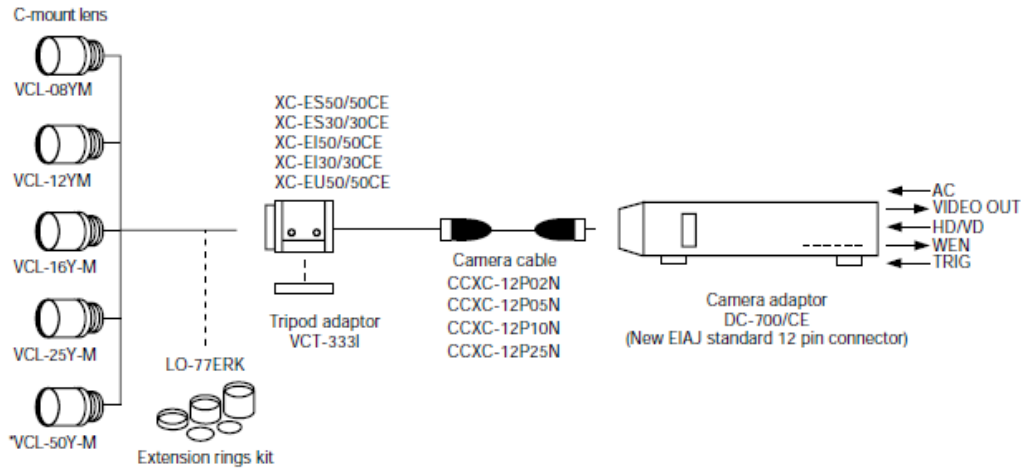
The three Series - XC-ES, XC-EI and XC-EU Series - differ in their applicable wavelength range so as to suit various environments of customer's site. The XC-ES Series (XC-ES50/ES50CE and XC-ES30/ES30CE) are standard models for visible radiation range, while the XC-EI Series cameras (XC-EI50/EI50CE and XC-EI30/EI30CE) are near IR models which have near-infrared sensitivity. When used with an IR LED illuminator, the XC-EI cameras can capture clear images in very low light environments. On the other hand, the XC-EU Series (XC-EU 50/EU50CE) are UV models which can detect very detailed data, utilizing the characteristics of the shorter wavelength range, with the sensitivity to the near-ultraviolet range (365 nm).

All models have identical dimensions and controls, making them easy to interchange. A variety of settings are available for differing subject and lighting conditions. All camera control switches are accessible from the outside of the camera. Excellent vibration and shock characteristics make these cameras ideal for demanding machine vision applications.

FEATURES

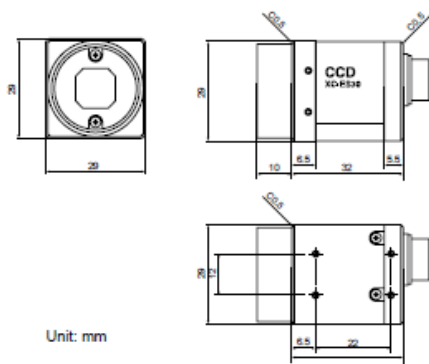
- XC-ES50/ES50CE/EI50/EI50CE: 1/2-inch type IT CCD
- XC-ES30/ES30CE/EI30/EI30CE: 1/3-inch type IT CCD
- XC-EU50/EU50CE: 1/2-inch type IT CCD
- Compact and light weight: 29 (W) x 29 (H) x 32 (D) mm, 50 g (1³/₁₆ x 1³/₁₆ x 1⁵/₁₆ inches, 2 oz)
- Near-infrared sensitivity (XC-EI50/EI50CE, XC-EI30/EI30CE)
- Near-ultraviolet sensitivity (XC-EU50/EU50CE)
- Minimum illumination at F1.4
 - 0.3 lx (XC-ES50/ES50CE, XC-ES30/ES30CE)
 - 0.1 lx (XC-EI50/EI50CE)
 - 0.2 lx (XC-EI30/EI30CE)
- High S/N Ratio: 60 dB
- Electronic shutter function (1/100 - 1/10,000 s)
- Flexible trigger shutter function
- 2:1 interlaced/non-interlaced
- Frame/field exposure
- Restart/reset function
- Synchronization: internal/external (HD/VD, VS)
- High shock and vibration tolerance

CONNECTION DIAGRAM

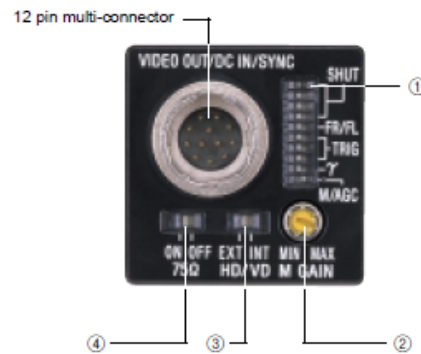


*Only VCL-50Y-M is applicable to the XC-EU50.

DIMENSIONS & REAR PANEL



Unit: mm



12 Pin multi-connector



PIN No.	External sync (HD/VD)	Internal sync (HD/VD)
1	GND	GND
2	+12 V	+12 V
3	GND	GND
4	Video output	Video output
5	GND	GND
6	*1 HD input	HD output
7	*1 VD input	VD output
8	GND	GND
9	-	-
10	*2 WEN output	*2 WEN output
11	TRIG Input	TRIG input
12	GND	GND

*1 HD/VD input is required when using restart, reset mode.
*2 WEN output works only when in external trigger shutter mode.

● Factory setting mode of rear panel

No.	Switch name	Factory-setting mode	
①	Shutter speed/Mode setting DIP switch	Dip switch 1-4: Shutter speed	OFF
		Dip switch 5: FRAME/FIELD	FRAME
		Dip switch 6-8: External trigger shutter mode, restart/reset mode	Normal
		Dip switch 9: Gamma ON/OFF	OFF
		Dip switch 0: GAIN	Manual
②	Manual GAIN (M GAIN) control knob	Twelve o'clock position	
③	HD/VD signal input/output switch	EXT	
④	75 Ω termination switch	ON	

ACCESSORIES

Compact camera adaptor DC-700/700CE

- Compact, lightweight (700 g, 1 lb 8 oz)
- External sync IN / OUT
- Trigger input / WEN output
- New EIAJ standard 12 pin connector
- Dimensions: 110(W) x 53(H) x 160(D) mm (4 3/8 x 2 1/8 x 6 3/8 inches)



12 pin camera cable (CE standard)

- CCXC-12P02N (2m)
- CCXC-12P05N (5m)
- CCXC-12P10N (10m)
- CCXC-12P25N (25m)



Tripod adaptor VCT-333I

- ABS
- Approx. 6.1 g (0.2 oz)
- Dimensions: 18(W)x6(H)x2.9(D)mm (23/32 x 1/4 x 1/8 inches)



Standard model

XC-ES50/ES50CE XC-ES30/ES30CE



Near IR model

XC-EI50/EI50CE XC-EI30/EI30CE



■ Applicable wavelength range



■ Applicable wavelength range



SPECIFICATIONS

	XC-ES50	XC-ES50CE	XC-ES30	XC-ES30CE	XC-EI50	XC-EI50CE	XC-EI30	XC-EI30CE
Image device	1/2 type IT CCD		1/2 type IT CCD		1/2 type IT CCD		1/2 type IT CCD	
Effective picture elements	768(H) x 494(V)	752(H) x 582(V)	768(H) x 494(V)	752(H) x 582(V)	768(H) x 494(V)	752(H) x 582(V)	768(H) x 494(V)	752(H) x 582(V)
Signal system	EIA (standard)	CCIR (standard)	EIA (standard)	CCIR (standard)	EIA (standard)	CCIR (standard)	EIA (standard)	CCIR (standard)
Horizontal frequency	15.734 kHz	15.652 kHz	15.734 kHz	15.652 kHz	15.734 kHz	15.652 kHz	15.734 kHz	15.652 kHz
Vertical frequency	59.94 Hz	50 Hz	59.94 Hz	50 Hz	59.94 Hz	50 Hz	59.94 Hz	50 Hz
Cell Size	8.4 x 9.8 μm	8.6 x 8.3 μm	6.35 x 7.4 μm	6.5 x 6.25 μm	8.4 x 9.8 μm	8.6 x 8.3 μm	6.35 x 7.4 μm	6.5 x 6.25 μm
Lens mount	C mount							
Flange back	17.526 mm							
Sync system	Internal / External (auto)							
External sync system	HD / VD (2 to 5 Vp-p), VS							
External sync frequency	±1%							
Jitter	Less than ±50 nsec							
Scanning system	2:1 Interlaced							
Video output	1.0 Vp-p, negative, 75 Ω unbalanced							
Horizontal resolution	570 TV lines	560 TV lines	570 TV lines	560 TV lines	570 TV lines	560 TV lines	570 TV lines	560 TV lines
Sensitivity	400 lx F5.5 (γ = ON MIN GAIN, NO IR cut filter)		400 lx F4 (γ = ON MIN GAIN, NO IR cut filter)		400 lx F11 (γ = ON MIN GAIN, NO IR cut filter)		400 lx F8 (γ = ON MIN GAIN, NO IR cut filter)	
Minimum illumination*	0.3 lx		0.3 lx		0.1 lx		0.2 lx	
S/N ratio	60 dB							
Gain	AGC (0-18 dB) / Manual (0-18 dB) Selectable							
Gamma	ON / OFF							
Normal shutter	1/100 to 1/10,000 s	1/120 to 1/10,000 s	1/100 to 1/10,000 s	1/120 to 1/10,000 s	1/100 to 1/10,000 s	1/120 to 1/10,000 s	1/100 to 1/10,000 s	1/120 to 1/10,000 s
External trigger shutter**	1/4 to 1/10,000 s	1/4 to 1/8,000 s	1/4 to 1/10,000 s	1/4 to 1/8,000 s	1/4 to 1/10,000 s	1/4 to 1/8,000 s	1/4 to 1/10,000 s	1/4 to 1/8,000 s
Power requirements	DC12 V (+9 to 16 V)							
Power consumption	1.5 W		1.4 W		1.6 W		1.4 W	
Dimensions	29 (W) x 29 (H) x 32 (D) mm (1 1/16 x 1 1/16 x 1 1/16 inches)							
Mass	50 g (2 oz)							
Operation temp./mois.	-10 to +50°C (14 to +122°F) / 20 to 80%							
Storage temp./mois.	-20 to +60°C (-4 to +140°F) / 20 to 95%							
Vibration	10 G (20 to 200 Hz)							
Shock resistance	70 G							
Regulatory compliance	UL1492, FCC Class A Digital Device, CE (EN50081-2 + EN50082-2), AS4251.1 + AS4252.2							
Supplied accessories	Lens mount cap (1), Operating Instructions (1)							

* (F1.4, AGC ON, without IR cut filter) ** Using Dip switch on the rear panel or Using trigger pulse width

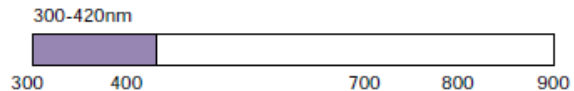
UV model

The XC-EU50/EU50P are compact, light-weight CCD cameras which have near-ultraviolet sensitivity with peak around 365 nm. Utilizing the shorter wavelength range characteristic, these models can capture very detailed images. They are effective in capturing surfaces of various kinds of materials and are also ideal for capturing 3D images of flat objects. With the use of ultraviolet lighting, even details such as small scratches, dust or blemishes, which can be undetected by the human eyes, can be clearly captured by these cameras.

XC-EU50/EU50CE



■ Applicable wavelength range



SPECIFICATIONS

	XC-EU50	XC-EU50CE
Image device	1/2 type IT CCD	
Signal system	EIA	CCIR
Effective picture elements	768 x 494	752 x 582
Cell size	8.4 (H) x 9.8 (V) μm	8.6 (H) x 8.3 (V) μm
Horizontal frequency	15.734 kHz	15.625 kHz
Vertical frequency	59.94 Hz	50 Hz
Lens mount	C mount	
Flange back	17.526 mm	
Sync system	Internal / External (auto)	
External sync system	HD / VD (2 to 5 Vp-p), VS	
External sync frequency	±1%	
Jitter	Less than ±50 nsec	
Scanning system	2:1 Interlaced	
Video output	1.0 Vp-p, negative, 75 Ω unbalanced	
Horizontal resolution	570 TV lines	560 TV lines
S/N ratio	60 dB	
Gain	AGC / Manual Selectable	
Gamma	ON / OFF	
Normal shutter	1/100 to 1/10,000 s	1/100 to 1/10,000 s
External trigger shutter	1/4 to 1/10,000 s	1/4 to 1/10,000 s
Power requirements	DC12 V (+9 to 16 V)	
Power consumption	1.6 W	
Dimensions	29 (W) x 29 (H) x 32 (D) mm (1 1/8 x 1 1/8 x 1 3/8 inches)	
Mass	50 g (2 oz)	
Operation temp./mois.	-5 to +45°C (-23 to +113°F) / 20 to 80% (no condensing)	
Storage temp./mois.	-20 to +50°C (-4 to +122°F) / 20 to 95% (no condensing)	
Vibration	10 G (20 to 200 Hz)	
Shock resistance	70 G	
Regulatory compliance	UL1492, FCC Class A Digital Device, CE (EN50081-2 + EN50082-2), EMC (AS35448)	
Supplied accessories	Lens mount cap (1), Operating instructions (1)	

Product information is available on the ISP Home Page

Sony online <http://www.sony.co.jp/ISP/>

Click!

Product Information

Information including product features and catalogs

Document & Software

Product document information and sample software downloads

Product catalog

User's Guide
XC-E series
XC-EU50/EU50CE

Application Guide

Instruction Manual

Command List

Sample software

● Sony Electronics Inc. (USA) HQ

1 Sony Drive Park Ridge, NJ 07656

(TEL:+1-800-686-7669)

<http://www.sony.com/videocameras>

(TEL:+1-416-499-1414)

(FAX:+1-416-497-1774)

(TEL:+31-20-44-99-351)

(FAX:+31-20-44-99-333)

<http://www.sony-vision.com>

(TEL:+49-221-537-8923)

(FAX:+49-221-537-491)

(TEL:+33-1-55-90-41-58)

(FAX:+33-1-55-90-42-20)

(TEL:+44-990-331122)

(FAX:+44-1932-817011)

(TEL:+46-40-190-800)

(FAX:+46-40-190-450)

(TEL:+39-02-61-83-64-26)

(FAX:+39-02-618-38-402)

● Sony of Canada Ltd. (CANADA)

115 Gordon Baker Rd, Toronto, Ontario M2H 3R5

● Sony Broadcast & Professional Europe HQ

Schliphofweg 275 1171 PK Badhoevedorp The Netherlands

Germany

Hugo-Eckener-Strasse 20 D-50829 Köln

France

15-26 rue Morel 92110 Clichy

UK

The Heights, Brooklands, Weybridge, Surrey KT13 0XW

Nordic

Per Albin Hanssons väg 20 S-214 32 Malmö Sweden

Italy

Via Galileo Galilei 40 I-20092 Cinisello Balsamo, Milano

MK7726V1IW01JUN

©2001 Sony Corporation. All rights reserved.
Reproduction in whole or in part without written permission is prohibited.
Design and specifications are subject to change without notice.
Printed in Japan on recycled paper.

COMPUTAR TEC-55

computar

TEC-55

55mm F2.8
for 2/3" format cameras
C-Mount

Machine Vision
Microscope Lens

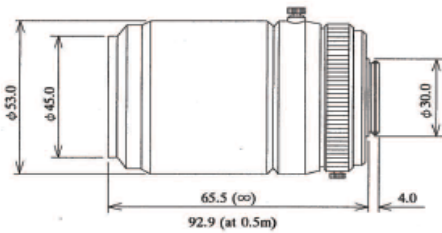
Model No.	TEC-M55	Effective	Front	φ33.0 mm
Focal Length	55 mm	Lens Aperture	Rear	φ13.3 mm
Max. Aperture Ratio	1 : 2.8	Back Focal Length		29.8 mm
Max. Image Format	8.8 X 6.6 mm (φ11 mm)	Flange Back Length		17.526 mm
Operation	Iris	F2.8 ~ 32C	Mount	C-Mount
	Focus	Manual,(0.14~Inf.)	Filter Size	M43 X 0.75mm
Object Distance at M.O.D.	17 X 13mm	Dimensions		φ53.0 X 92.9mm
		Weight		320 g
Angle of View	D			11.5°
	H	2/3"		9.2°
	V			6.9°

2/3

C

M.O.D. : Minimum Object Distance

Dimensions



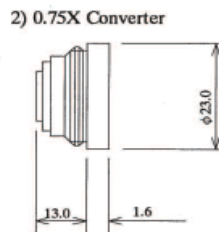
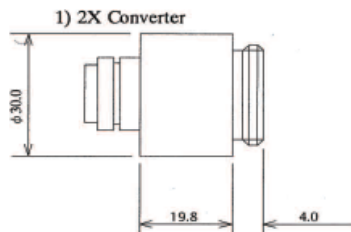
When using Optical accessories, Please remove (Screw-out) Dust-Proof cover glass.

f = 55 mm

Object Distance	Object Size (Horizontal)	
	2/3" Format	1/2" Format
5,000 mm	700 mm	550 mm
3,000	400	320
1,000	150	120
500	70	53
300	40	32
200	27	20
140	17	12

Object Distance : Distance from Lens surface to Object
Object Size : Full Size appeared on Monitor

Optional Accessories



SP

Subject to change without notice

Printed in Japan

Mar. '97

IR-Lumineszenzdiode (850 nm) mit hoher Ausgangsleistung
High Power Infrared Emitter (850 nm)
Lead (Pb) Free Product - RoHS Compliant
SFH 4550



Wesentliche Merkmale

- Infrarot LED mit hoher Ausgangsleistung
- Enger Abstrahlwinkel $\pm 3^\circ$
- Sehr hohe Strahlstärke
- Kurze Schaltzeiten
- UL Version erhältlich

Anwendungen

- Infrarotbeleuchtung für Kameras
- Sensorik
- Datenübertragung
- Rauchmelder

Sicherheitshinweise

Je nach Betriebsart emittieren diese Bauteile hochkonzentrierte, nicht sichtbare Infrarot-Strahlung, die gefährlich für das menschliche Auge sein kann. Produkte, die diese Bauteile enthalten, müssen gemäß den Sicherheitsrichtlinien der IEC-Normen 60825-1 und 62471 behandelt werden.

Features

- High Power Infrared LED
- Narrow emission angle $\pm 3^\circ$
- Very high radiant intensity
- Short switching times
- UL version available

Applications

- Infrared illumination for cameras
- Sensor technology
- Data transmission
- Smoke detectors

Safety Advices

Depending on the mode of operation, these devices emit highly concentrated non visible infrared light which can be hazardous to the human eye. Products which incorporate these devices have to follow the safety precautions given in IEC 60825-1 and IEC 62471.

Typ Type	Bestellnummer Ordering Code	Strahlstärkegruppierung ¹⁾ ($I_F = 100 \text{ mA}$, $t_p = 20 \text{ ms}$) Radiant Intensity Grouping ¹⁾ I_e (mW/sr)
SFH 4550	Q65110A1772	≥ 400 (typ. 700)

¹⁾ gemessen bei einem Raumwinkel $\Omega = 0.001 \text{ sr}$ / measured at a solid angle of $\Omega = 0.001 \text{ sr}$

Grenzwerte ($T_A = 25\text{ °C}$)
Maximum Ratings

Bezeichnung Parameter	Symbol Symbol	Wert Value	Einheit Unit
Betriebs- und Lagertemperatur Operating and storage temperature range	T_{op}, T_{stg}	- 40 ... + 100	°C
Sperrspannung Reverse voltage	V_R	5	V
Vorwärtsgleichstrom Forward current	I_F	100	mA
Stoßstrom, $t_p = 10\ \mu\text{s}$, $D = 0$ Surge current	I_{FSM}	1.5	A
Verlustleistung Power dissipation	P_{tot}	180	mW
Wärmewiderstand Sperrschicht - Umgebung bei Montage auf FR4 Platine, Padgröße je $16\ \text{mm}^2$ Thermal resistance junction - ambient mounted on PC-board (FR4), padsize $16\ \text{mm}^2$ each	R_{thJA}	450	K/W

Kennwerte ($T_A = 25\text{ °C}$)
Characteristics

Bezeichnung Parameter	Symbol Symbol	Wert Value	Einheit Unit
Wellenlänge der Strahlung Wavelength at peak emission $I_F = 100\ \text{mA}$	λ_{peak}	860	nm
Centroid-Wellenlänge der Strahlung Centroid wavelength $I_F = 100\ \text{mA}$	$\lambda_{centroid}$	850	nm
Spektrale Bandbreite bei 50% von I_{max} Spectral bandwidth at 50% of I_{max} $I_F = 100\ \text{mA}$	$\Delta\lambda$	42	nm
Abstrahlwinkel Half angle	φ	± 3	Grad deg.
Aktive Chipfläche Active chip area	A	0.09	mm^2
Abmessungen der aktiven Chipfläche Dimension of the active chip area	$L \times B$ $L \times W$	0.3×0.3	mm^2

Kennwerte ($T_A = 25\text{ °C}$)
Characteristics (cont'd)

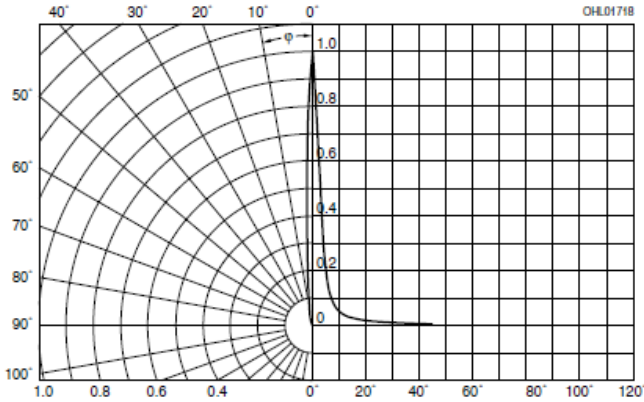
Bezeichnung Parameter	Symbol Symbol	Wert Value	Einheit Unit
Schaltzeiten, I_a von 10% auf 90% und von 90% auf 10%, bei $I_F = 100\text{ mA}$, $R_L = 50\ \Omega$ Switching times, I_a from 10% to 90% and from 90% to 10%, $I_F = 100\text{ mA}$, $R_L = 50\ \Omega$	t_r , t_f	12	ns
Durchlassspannung Forward voltage $I_F = 100\text{ mA}$, $t_p = 20\text{ ms}$ $I_F = 1\text{ A}$, $t_p = 100\ \mu\text{s}$	V_F V_F	1.5 (< 1.8) 2.4 (< 3.0)	V V
Sperrstrom Reverse current	I_R	not designed for reverse operation	μA
Gesamtstrahlungsfluss Total radiant flux $I_F = 100\text{ mA}$, $t_p = 20\text{ ms}$	Φ_e typ	50	mW
Temperaturkoeffizient von I_a bzw. Φ_e , $I_F = 100\text{ mA}$ Temperature coefficient of I_a or Φ_e , $I_F = 100\text{ mA}$	TC_I	- 0.5	%/K
Temperaturkoeffizient von V_F , $I_F = 100\text{ mA}$ Temperature coefficient of V_F , $I_F = 100\text{ mA}$	TC_V	- 0.7	mV/K
Temperaturkoeffizient von λ , $I_F = 100\text{ mA}$ Temperature coefficient of λ , $I_F = 100\text{ mA}$	TC_λ	+ 0.3	nm/K

Strahlstärke I_e in Achsrichtung¹⁾
 gemessen bei einem Raumwinkel $\Omega = 0.001$ sr
Radiant Intensity I_e in Axial Direction
 at a solid angle of $\Omega = 0.001$ sr

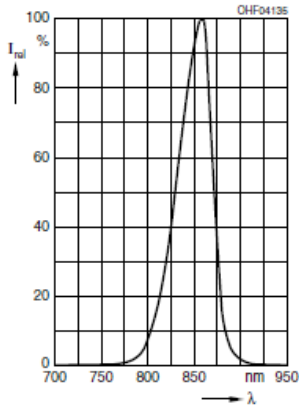
Bezeichnung Parameter	Symbol	Werte Values			Einheit Unit
		SFH 4550-DW	SFH 4550-EW	SFH 4550-FW	
Strahlstärke Radiant intensity $I_F = 100$ mA, $t_p = 20$ ms	$I_{e \text{ min}}$ $I_{e \text{ max}}$	400 800	630 1250	1000 2000	mW/sr mW/sr
Strahlstärke Radiant intensity $I_F = 1$ A, $t_p = 100$ μ s	$I_{e \text{ typ}}$	5000	7000	9000	mW/sr

¹⁾ Nur eine Gruppe in einer Verpackungseinheit (Streuung kleiner 2:1) /
 Only one group in one packing unit (variation lower 2:1)

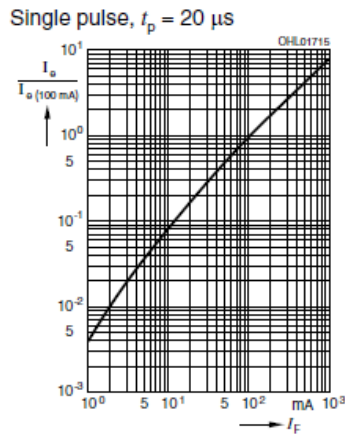
Abstrahlcharakteristik
Radiation Characteristics $I_{rel} = f(\varphi)$



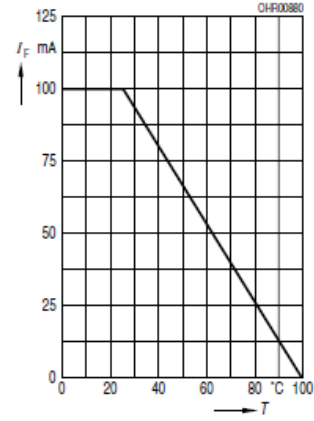
Relative Spectral Emission
 $I_{rel} = f(\lambda)$



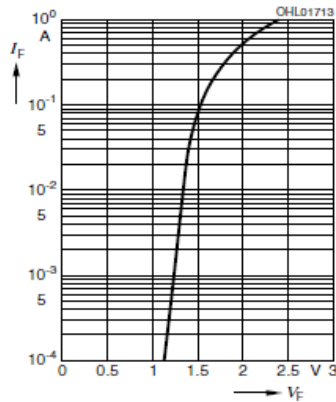
Radiant Intensity $\frac{I_a}{I_a(100 \text{ mA})} = f(I_F)$



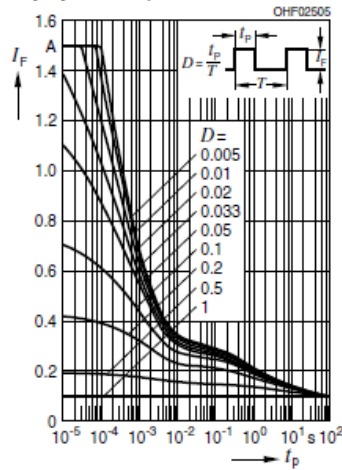
Max. Permissible Forward Current
 $I_F = f(T_A), R_{thJA} = 450 \text{ K/W}$



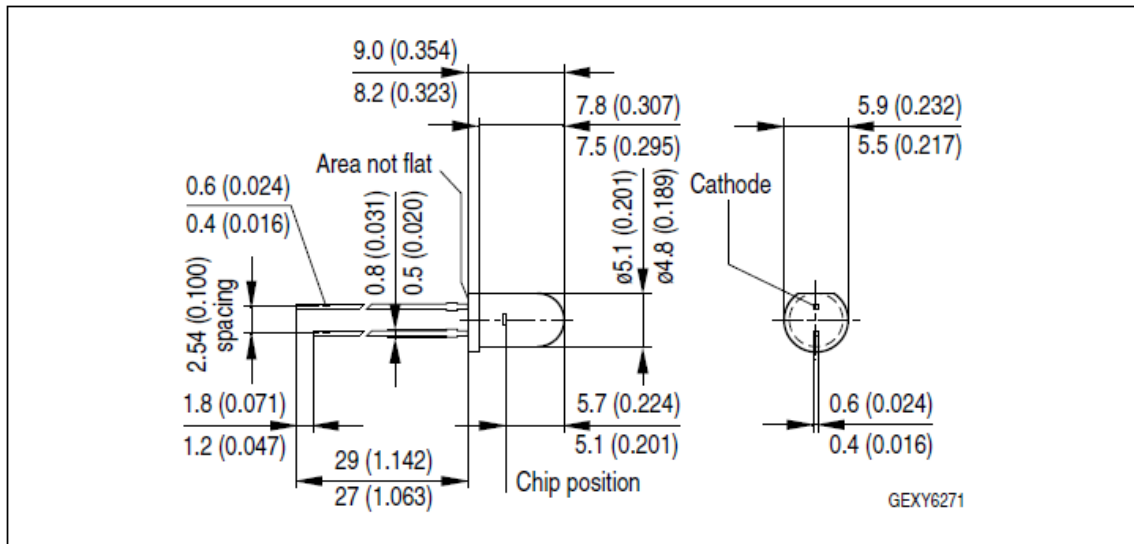
Forward Current $I_F = f(V_F)$
 Single pulse, $t_p = 20 \mu\text{s}$



Permissible Pulse Handling Capability $I_F = f(\tau), T_A = 25 \text{ }^\circ\text{C}$,
 duty cycle $D = \text{parameter}$



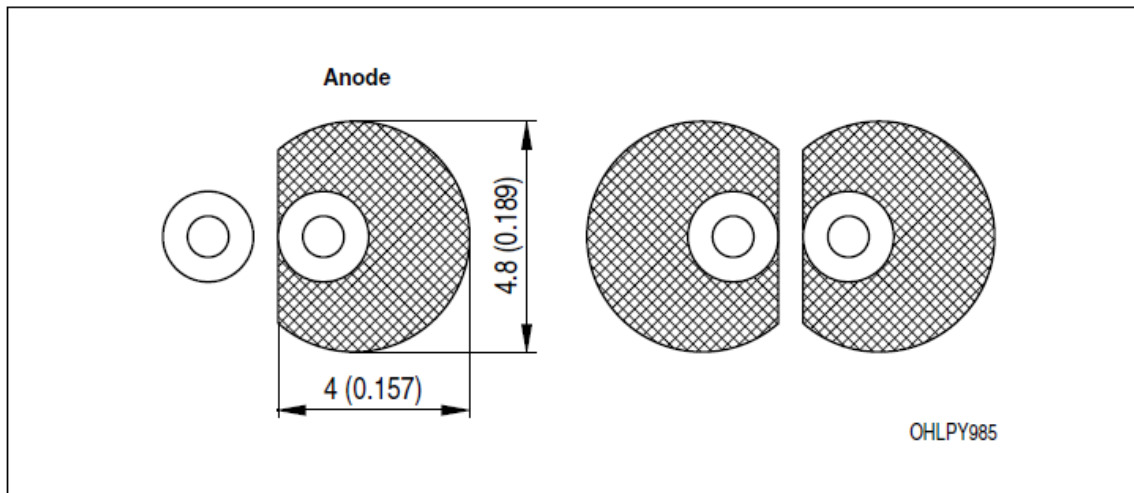
Maßzeichnung
Package Outlines



Maße in mm (inch) / Dimensions in mm (inch).

Empfohlenes Lötpaddesign
Recommended Solder Pad Design

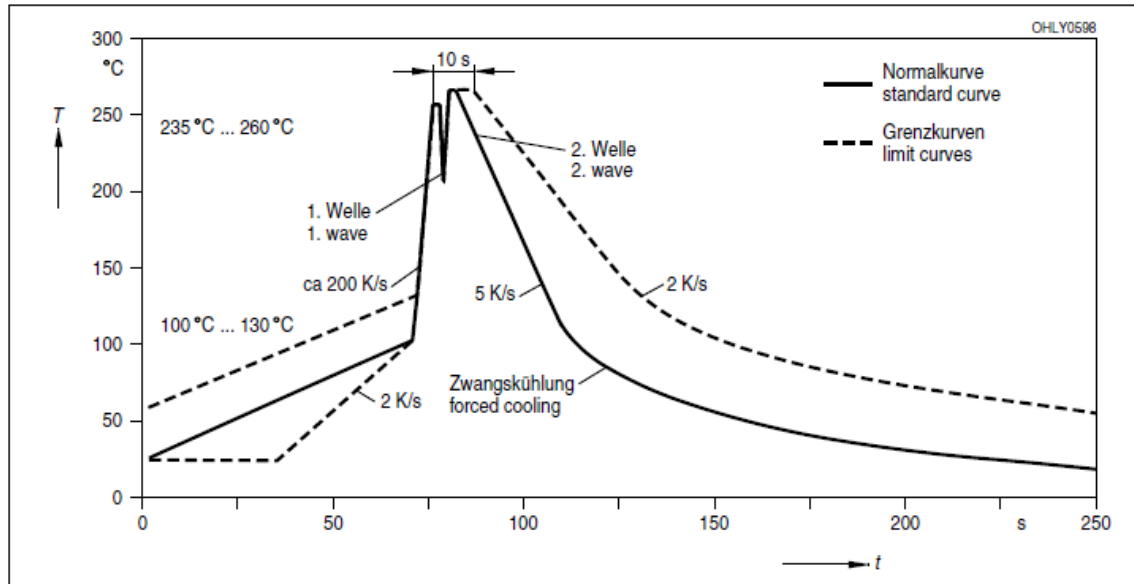
Wellenlöten TTW
TTW Soldering



Maße in mm (inch) / Dimensions in mm (inch).

Lötbedingungen
Soldering Conditions
Wellenlöten (TTW)
TTW Soldering

(nach CECC 00802)
 (acc. to CECC 00802)



Published by
OSRAM Opto Semiconductors GmbH
 Leibnizstraße 4, D-93055 Regensburg
www.osram-os.com
 © All Rights Reserved.

EU RoHS and China RoHS compliant product



此产品符合欧盟 RoHS 指令的要求；

按照中国的相关法规和标准，不含有毒有害物质或元素。

The information describes the type of component and shall not be considered as assured characteristics. Terms of delivery and rights to change design reserved. Due to technical requirements components may contain dangerous substances. For information on the types in question please contact our Sales Organization.

Packing

Please use the recycling operators known to you. We can also help you – get in touch with your nearest sales office. By agreement we will take packing material back, if it is sorted. You must bear the costs of transport. For packing material that is returned to us unsorted or which we are not obliged to accept, we shall have to invoice you for any costs incurred.

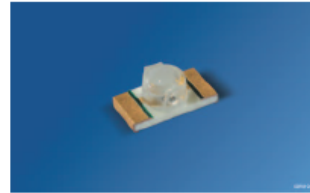
Components used in life-support devices or systems must be expressly authorized for such purpose! Critical components¹, may only be used in life-support devices or systems² with the express written approval of OSRAM OS.

¹ A critical component is a component used in a life-support device or system whose failure can reasonably be expected to cause the failure of that life-support device or system, or to affect its safety or effectiveness of that device or system.

² Life support devices or systems are intended (a) to be implanted in the human body, or (b) to support and/or maintain and sustain human life. If they fail, it is reasonable to assume that the health of the user may be endangered.

IR-Lumineszenzdiode (850 nm) mit hoher Ausgangsleistung
High Power Infrared Emitter (850 nm)
Lead (Pb) Free Product - RoHS Compliant

SFH 4058



Wesentliche Merkmale

- Sehr kleines Gehäuse:
(LxBxH) 3.2 mm x 1.6mm x 1.1 mm
- Sehr hohe Gesamtleistung

Anwendungen

- Miniaturlichtschranken
- Industrieelektronik
- „Messen/Steuern/Regeln“
- Sensorik

Sicherheitshinweise

Je nach Betriebsart emittieren diese Bauteile hochkonzentrierte, nicht sichtbare Infrarot-Strahlung, die gefährlich für das menschliche Auge sein kann. Produkte, die diese Bauteile enthalten, müssen gemäß den Sicherheitsrichtlinien der IEC-Normen 60825-1 und 62471 behandelt werden.

Features

- Very small package:
(LxWxH) 3.2 mm x 1.6 mm x 1.1 mm
- High optical total power

Applications

- Miniature photointerrupters
- Industrial electronics
- For drive and control circuits
- Sensor technology

Safety Advices

Depending on the mode of operation, these devices emit highly concentrated non visible infrared light which can be hazardous to the human eye. Products which incorporate these devices have to follow the safety precautions given in IEC 60825-1 and IEC 62471.

Typ Type	Bestellnummer Ordering Code	Strahlstärkegruppierung ¹⁾ ($I_F = 70 \text{ mA}$, $t_p = 20 \text{ ms}$) Radiant Intensity Grouping ¹⁾ I_e (mW/sr)
SFH 4058	Q65110A9218	≥ 6.3 (typ. 15)

¹⁾ gemessen bei einem Raumwinkel $\Omega = 0.01 \text{ sr}$ / measured at a solid angle of $\Omega = 0.01 \text{ sr}$

Grenzwerte ($T_A = 25\text{ °C}$)
Maximum Ratings

Bezeichnung Parameter	Symbol Symbol	Wert Value	Einheit Unit
Betriebs- und Lagertemperatur Operating and storage temperature range	T_{op}, T_{stg}	- 40 ... + 85	°C
Sperrspannung Reverse voltage	V_R	5	V
Vorwärtsgleichstrom Forward current	I_F	70	mA
Stoßstrom, $t_p = 10\text{ }\mu\text{s}$, $D = 0$ Surge current	I_{FSM}	700	mA
Verlustleistung Power dissipation	P_{tot}	140	mW
Wärmewiderstand Sperrschicht - Umgebung bei Montage auf FR4 Platine, Padgröße je 5 mm^2 Thermal resistance junction - ambient mounted on PC-board (FR4), padsize 5 mm^2 each	R_{thJA}	540	K/W
Wärmewiderstand Sperrschicht - Lötstelle bei Montage auf Metall-Block Thermal resistance junction - soldering point, mounted on metal block	R_{thJS}	360	K/W

Kennwerte ($T_A = 25\text{ °C}$)
Characteristics

Bezeichnung Parameter	Symbol Symbol	Wert Value	Einheit Unit
Wellenlänge der Strahlung Wavelength at peak emission $I_F = 70\text{ mA}$, $t_p = 10\text{ ms}$	λ_{peak}	860	nm
Schwerpunkts-Wellenlänge der Strahlung Centroid Wavelength $I_F = 70\text{ mA}$, $t_p = 10\text{ ms}$	$\lambda_{centroid}$	850	nm
Spektrale Bandbreite bei 50% von I_{max} Spectral bandwidth at 50% of I_{max} $I_F = 70\text{ mA}$, $t_p = 10\text{ ms}$	$\Delta\lambda$	42	nm
Abstrahlwinkel Half angle	φ	± 40	Grad deg.
Aktive Chipfläche Active chip area	A	0.04	mm^2

Kennwerte ($T_A = 25\text{ °C}$)
Characteristics (cont'd)

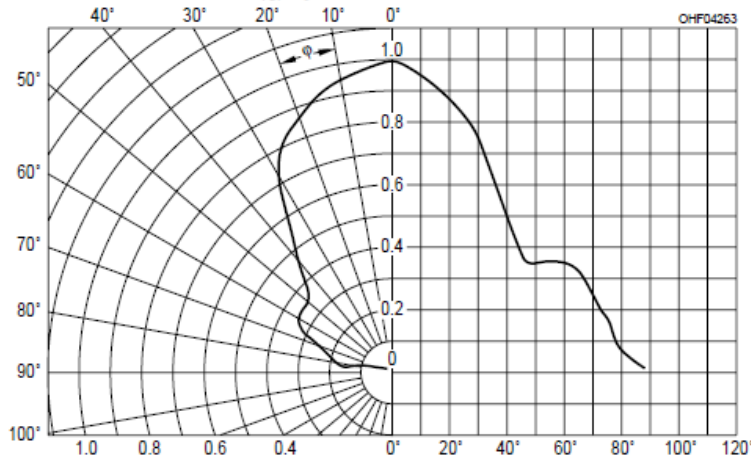
Bezeichnung Parameter	Symbol Symbol	Wert Value	Einheit Unit
Abmessungen der aktiven Chipfläche Dimension of the active chip area	$L \times B$ $L \times W$	0.2×0.2	mm ²
Schaltzeiten, I_e von 10% auf 90% und von 90% auf 10%, bei $I_F = 70\text{ mA}$, $R_L = 50\ \Omega$ Switching times, I_e from 10% to 90% and from 90% to 10%, $I_F = 70\text{ mA}$, $R_L = 50\ \Omega$	t_r , t_f	10	ns
Durchlassspannung Forward voltage $I_F = 70\text{ mA}$, $t_p = 20\text{ ms}$	V_F	1.6 (< 2.0)	V
Sperrstrom Reverse current	I_R	not designed for reverse operation	μA
Gesamtstrahlungsfluss Total radiant flux $I_F = 70\text{ mA}$, $t_p = 20\text{ ms}$	$\Phi_{e\text{ typ}}$	33	mW
Temperaturkoeffizient von I_e bzw. Φ_e , $I_F = 70\text{ mA}$ Temperature coefficient of I_e or Φ_e , $I_F = 70\text{ mA}$	TC_I	- 0.5	%/K
Temperaturkoeffizient von V_F , $I_F = 70\text{ mA}$ Temperature coefficient of V_F , $I_F = 70\text{ mA}$	TC_V	- 0.7	mV/K
Temperaturkoeffizient von λ , $I_F = 70\text{ mA}$ Temperature coefficient of λ , $I_F = 70\text{ mA}$	TC_λ	+ 0.3	nm/K

Strahlstärke I_e in Achsrichtung¹⁾
 gemessen bei einem Raumwinkel $\Omega = 0.01$ sr
Radiant Intensity I_e in Axial Direction
 at a solid angle of $\Omega = 0.01$ sr

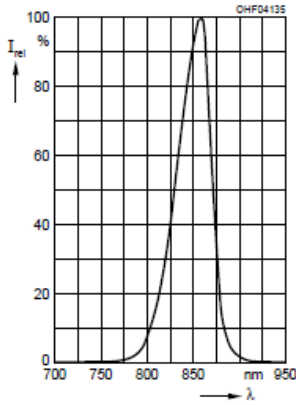
Bezeichnung Parameter	Symbol	Werte Values			Einheit Unit
		SFH 4058			
		-Q	-R	-S	
Strahlstärke Radiant intensity $I_F = 70$ mA, $t_p = 20$ ms	$I_{e \text{ min}}$ $I_{e \text{ max}}$	6.3 12.5	10 20	16 32	mW/sr mW/sr
Strahlstärke Radiant intensity $I_F = 500$ mA, $t_p = 25$ μ s	$I_{e \text{ typ}}$	36	55	90	mW/sr

¹⁾ Nur eine Gruppe in einer Verpackungseinheit (Streuung kleiner 2:1) /
 Only one bin in one packing unit (variation lower 2:1)

Abstrahlcharakteristik
Radiation Characteristics $I_{rel} = f(\varphi)$

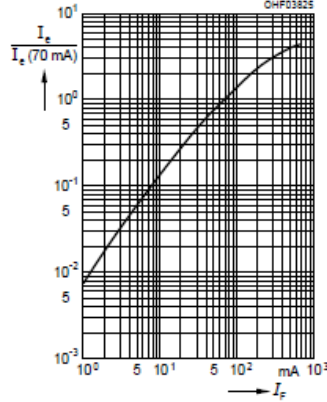


Relative Spectral Emission
 $I_{rel} = f(\lambda)$

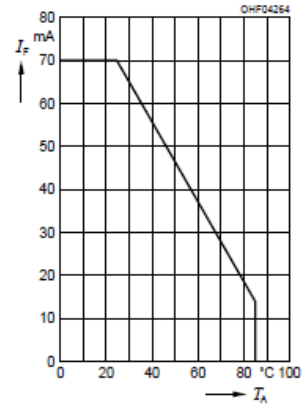


Radiant Intensity $\frac{I_e}{I_e 70 \text{ mA}} = f(I_F)$

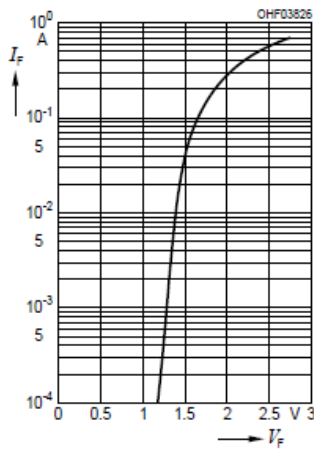
Single pulse, $t_p = 25 \mu\text{s}$



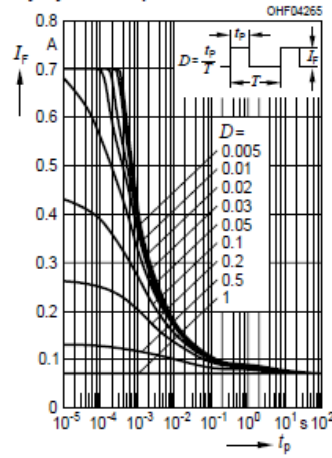
Max. Permissible Forward Current
 $I_F = f(T_A), R_{thJA} = 540 \text{ K/W}$



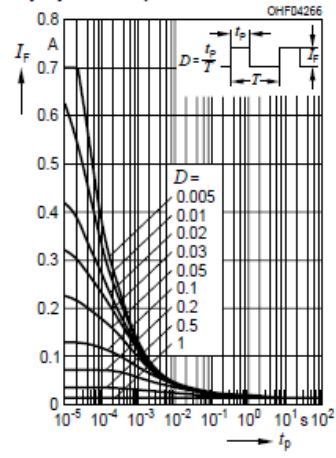
Forward Current $I_F = f(V_F)$
 Single pulse, $t_p = 100 \mu\text{s}$



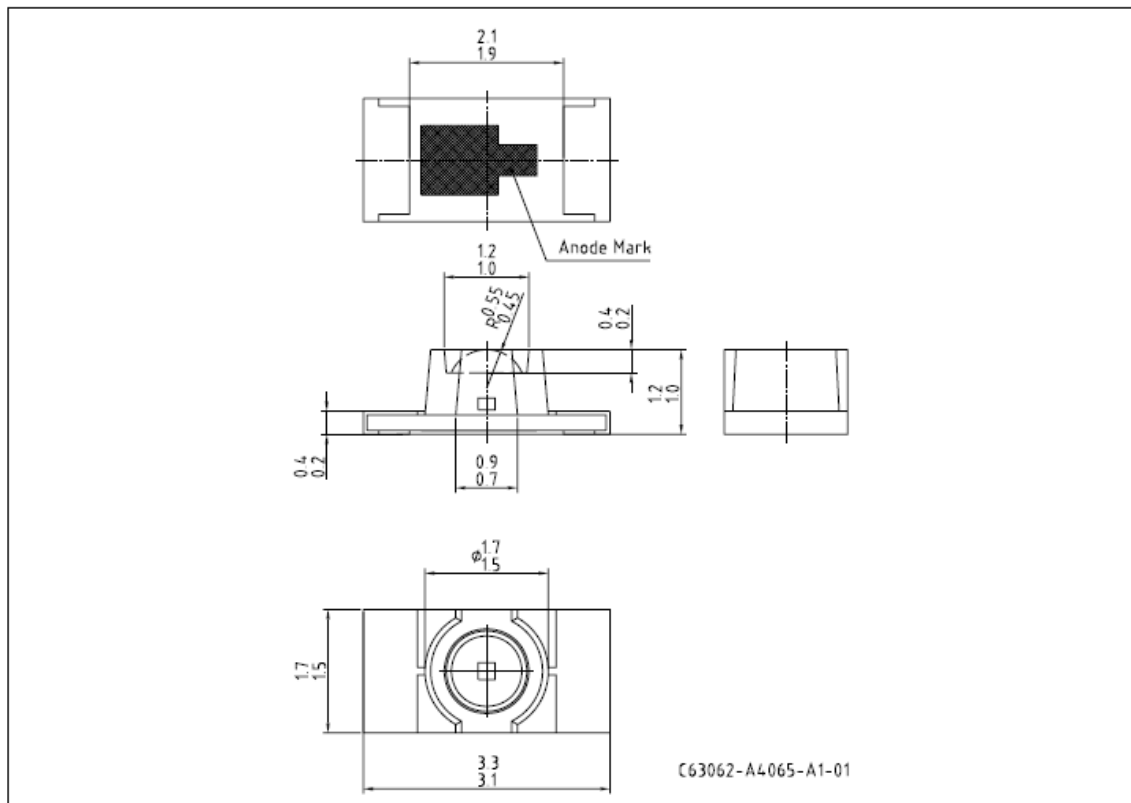
Permissible Pulse Handling Capability $I_F = f(\tau), T_A = 25 \text{ }^\circ\text{C}$,
 duty cycle $D = \text{parameter}$



Permissible Pulse Handling Capability $I_F = f(\tau), T_A = 85 \text{ }^\circ\text{C}$,
 duty cycle $D = \text{parameter}$



Maßzeichnung
Package Outlines



Maße in mm/ Dimensions in mm.

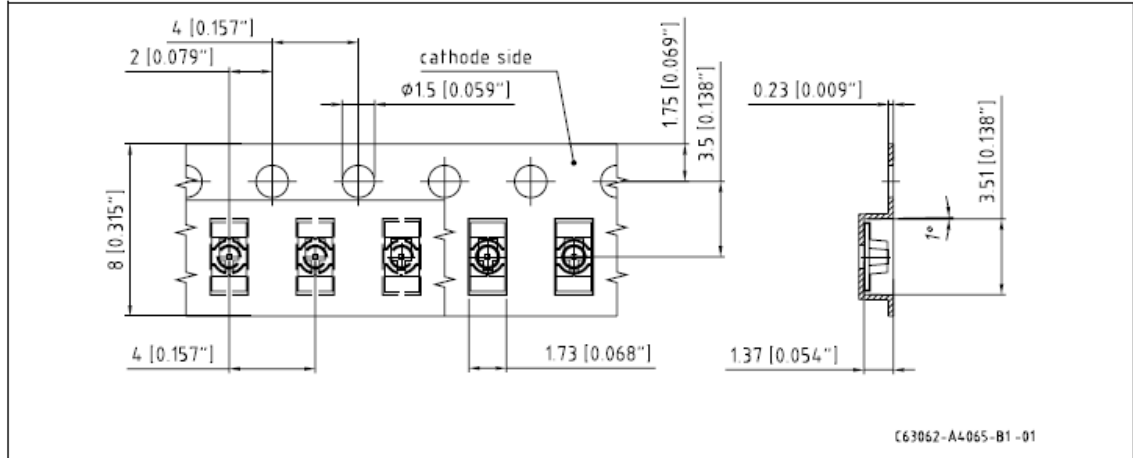
Gehäuse / Package	Chip LED/ Chip LED
Farbe / Colour	Farblos klar / colourless clear
Gehäusemarkierung/ Package marking	Anode / anode

Gurtung / Polarität und Lage

Verpackungseinheit 2000/Rolle, ø180 mm

Method of Taping / Polarity and Orientation

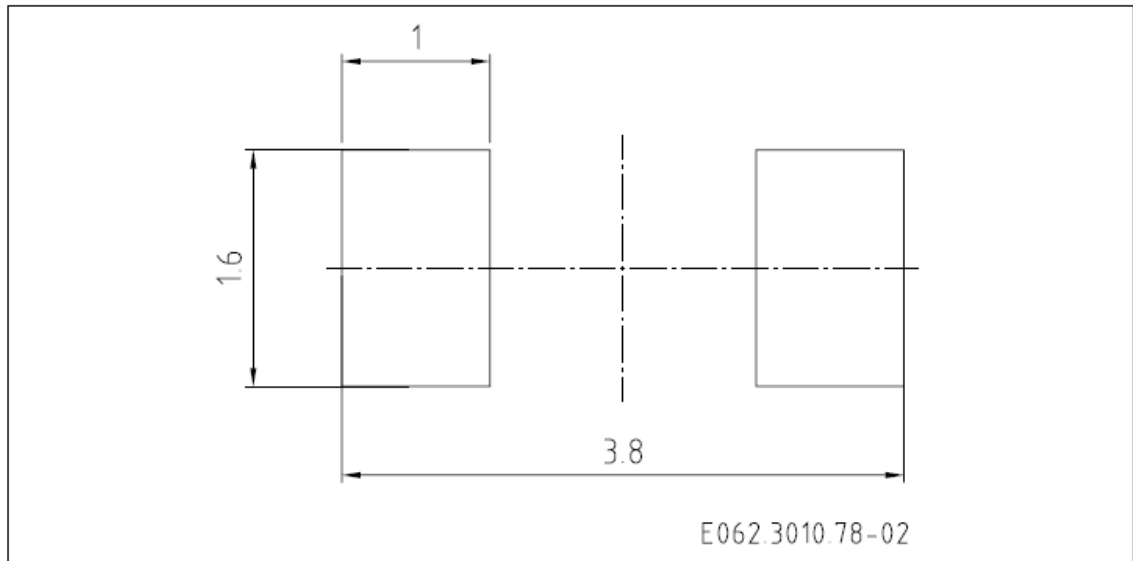
Packing unit 2000/reel, ø180 mm



Maße in mm (inch) / Dimensions in mm (inch).

**Empfohlenes Lötpaddingesign
Recommended Solder Pad**

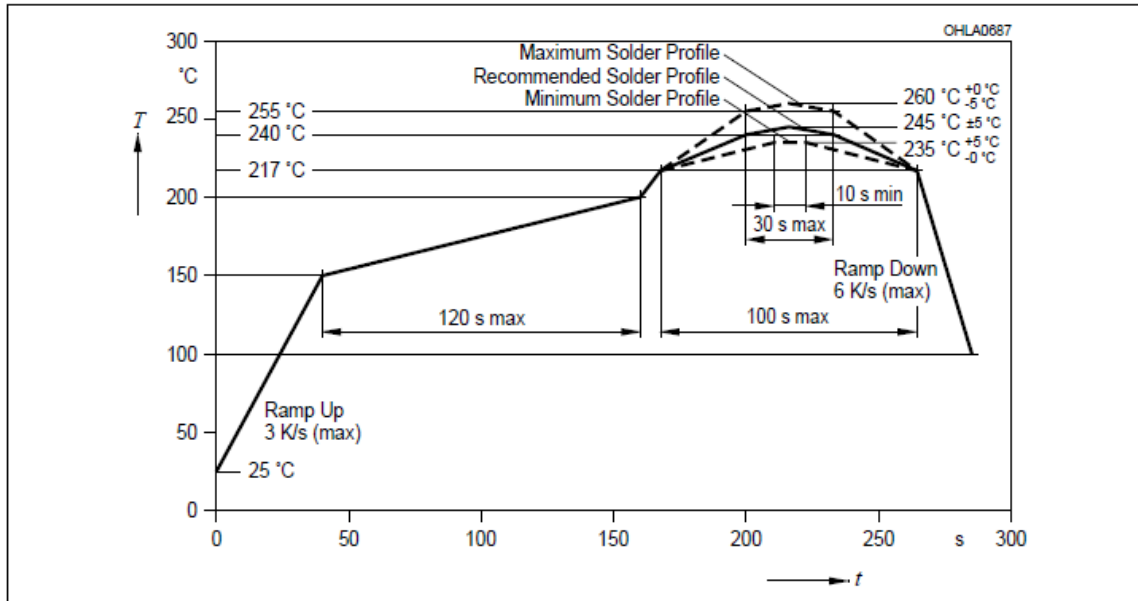
Reflow Lötén
Reflow Soldering



Maße in mm / Dimensions in mm.

Lötbedingungen
Soldering Conditions
Reflow Lötprofil für bleifreies Löten
Reflow Soldering Profile for lead free soldering

Vorbehandlung nach JEDEC Level 3
 Preconditioning acc. to JEDEC Level 3
 (nach J-STD-020C)
 (acc. to J-STD-020C)



Published by
OSRAM Opto Semiconductors GmbH
 Leibnizstrasse 4, D-93055 Regensburg
www.osram-os.com
 © All Rights Reserved.

The information describes the type of component and shall not be considered as assured characteristics. Terms of delivery and rights to change design reserved. Due to technical requirements components may contain dangerous substances. For information on the types in question please contact our Sales Organization.

Packing

Please use the recycling operators known to you. We can also help you – get in touch with your nearest sales office. By agreement we will take packing material back, if it is sorted. You must bear the costs of transport. For packing material that is returned to us unsorted or which we are not obliged to accept, we shall have to invoice you for any costs incurred.

Components used in life-support devices or systems must be expressly authorized for such purpose! Critical components¹, may only be used in life-support devices or systems² with the express written approval of OSRAM OS.

¹ A critical component is a component used in a life-support device or system whose failure can reasonably be expected to cause the failure of that life-support device or system, or to affect its safety or effectiveness of that device or system.

² Life support devices or systems are intended (a) to be implanted in the human body, or (b) to support and/or maintain and sustain human life. If they fail, it is reasonable to assume that the health of the user may be endangered.

EU RoHS and China RoHS compliant product



此产品符合欧盟 RoHS 指令的要求；

按照中国的相关法规和标准，不含有毒有害物质或元素。

IR-Lumineszenzdiode (850 nm) mit hoher Ausgangsleistung
High Power Infrared Emitter (850 nm)
Lead (Pb) Free Product - RoHS Compliant
SFH 4250



Wesentliche Merkmale

- Infrarot LED mit sehr hoher Ausgangsleistung
- Hohe Bestromung bei hohen Temperaturen möglich
- Kurze Schaltzeiten

Anwendungen

- Infrarotbeleuchtung für CMOS Kameras
- IR-Datenübertragung
- Sensorik

Sicherheitshinweise

Je nach Betriebsart emittieren diese Bauteile hochkonzentrierte, nicht sichtbare Infrarot-Strahlung, die gefährlich für das menschliche Auge sein kann. Produkte, die diese Bauteile enthalten, müssen gemäß den Sicherheitsrichtlinien der IEC-Normen 60825-1 und 62471 behandelt werden.

Features

- High Power Infrared LED
- High forward current allowed at high temperature
- Short switching times

Applications

- Infrared Illumination for CMOS cameras
- IR Data Transmission
- Optical sensors

Safety Advices

Depending on the mode of operation, these devices emit highly concentrated non visible infrared light which can be hazardous to the human eye. Products which incorporate these devices have to follow the safety precautions given in IEC 60825-1 and IEC 62471.

Typ Type	Bestellnummer Ordering Code	Strahlstärkegruppierung ¹⁾ ($I_F = 100 \text{ mA}$, $t_p = 20 \text{ ms}$) Radiant Intensity Grouping ¹⁾ I_e (mW/sr)
SFH 4250	Q65110A2465	≥ 10 (typ. 15)

¹⁾ gemessen bei einem Raumwinkel $\Omega = 0.01 \text{ sr}$ / measured at a solid angle of $\Omega = 0.01 \text{ sr}$

Grenzwerte ($T_A = 25\text{ °C}$)
Maximum Ratings

Bezeichnung Parameter	Symbol Symbol	Wert Value	Einheit Unit
Betriebs- und Lagertemperatur Operating and storage temperature range	T_{op}, T_{stg}	- 40 ... + 100	°C
Sperrspannung Reverse voltage	V_R	5	V
Vorwärtsgleichstrom Forward current	I_F	100	mA
Stoßstrom, $t_p = 100\text{ }\mu\text{s}$, $D = 0$ Surge current	I_{FSM}	1.5	A
Verlustleistung Power dissipation	P_{tot}	180	mW
Wärmewiderstand Sperrschicht - Umgebung bei Montage auf FR4 Platine, Padgröße je 16 mm ² Thermal resistance junction - ambient mounted on PC-board (FR4), padsize 16 mm ² each	R_{thJA}	300	K/W
Wärmewiderstand Sperrschicht - Lötstelle bei Montage auf Metall-Block Thermal resistance junction - soldering point, mounted on metal block	R_{thJS}	140	K/W

Kennwerte ($T_A = 25\text{ °C}$)
Characteristics

Bezeichnung Parameter	Symbol Symbol	Wert Value	Einheit Unit
Wellenlänge der Strahlung Wavelength at peak emission $I_F = 100\text{ mA}$	λ_{peak}	860	nm
Centroid-Wellenlänge der Strahlung Centroid wavelength $I_F = 100\text{ mA}$	$\lambda_{centroid}$	850	nm
Spektrale Bandbreite bei 50% von I_{max} Spectral bandwidth at 50% of I_{max} $I_F = 100\text{ mA}$	$\Delta\lambda$	42	nm
Abstrahlwinkel Half angle	φ	± 60	Grad deg.
Aktive Chipfläche Active chip area	A	0.09	mm ²

Kennwerte ($T_A = 25\text{ °C}$)
Characteristics (cont'd)

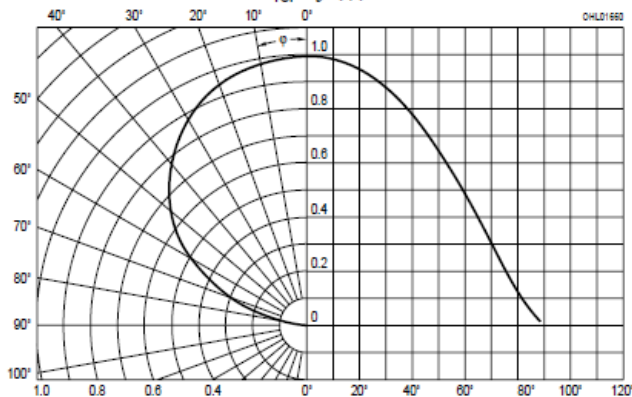
Bezeichnung Parameter	Symbol Symbol	Wert Value	Einheit Unit
Abmessungen der aktiven Chipfläche Dimension of the active chip area	$L \times B$ $L \times W$	0.3×0.3	mm ²
Schaltzeiten, I_e von 10% auf 90% und von 90% auf 10%, bei $I_F = 100\text{ mA}$, $R_L = 50\ \Omega$ Switching times, I_e from 10% to 90% and from 90% to 10%, $I_F = 100\text{ mA}$, $R_L = 50\ \Omega$	t_r , t_f	12	ns
Durchlassspannung Forward voltage $I_F = 100\text{ mA}$, $t_p = 20\text{ ms}$ $I_F = 1\text{ A}$, $t_p = 100\ \mu\text{s}$	V_F V_F	1.5 (< 1.8) 2.4 (< 3.0)	V V
Sperrstrom Reverse current	I_R	not designed for reverse operation	μA
Gesamtstrahlungsfluss Total radiant flux $I_F = 100\text{ mA}$, $t_p = 20\text{ ms}$	$\Phi_{e\text{ typ}}$	45	mW
Temperaturkoeffizient von I_e bzw. Φ_e , $I_F = 100\text{ mA}$ Temperature coefficient of I_e or Φ_e , $I_F = 100\text{ mA}$	TC_I	- 0.5	%/K
Temperaturkoeffizient von V_F , $I_F = 100\text{ mA}$ Temperature coefficient of V_F , $I_F = 100\text{ mA}$	TC_V	- 0.7	mV/K
Temperaturkoeffizient von λ , $I_F = 100\text{ mA}$ Temperature coefficient of λ , $I_F = 100\text{ mA}$	TC_λ	+ 0.3	nm/K

Strahlstärke I_e in Achsrichtung¹⁾
 gemessen bei einem Raumwinkel $\Omega = 0.01$ sr
Radiant Intensity I_e in Axial Direction
 at a solid angle of $\Omega = 0.01$ sr

Bezeichnung Parameter	Symbol	Werte Values		Einheit Unit
		SFH 4250-R	SFH 4250-S	
Strahlstärke Radiant intensity $I_F = 100$ mA, $t_p = 20$ ms	$I_{e \text{ min}}$ $I_{e \text{ max}}$	10 20	16 32	mW/sr mW/sr
Strahlstärke Radiant intensity $I_F = 1$ A, $t_p = 100$ μ s	$I_{e \text{ typ}}$	100	140	mW/sr

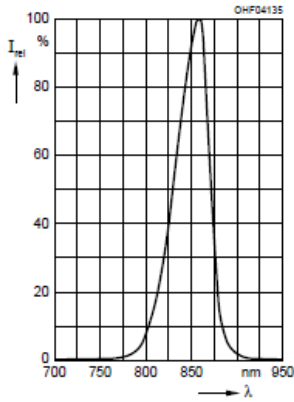
¹⁾ Nur eine Gruppe in einer Verpackungseinheit (Streuung kleiner 2:1) /
 Only one group in one packing unit (variation lower 2:1)

Abstrahlcharakteristik
Radiation Characteristics $I_{rel} = f(\varphi)$



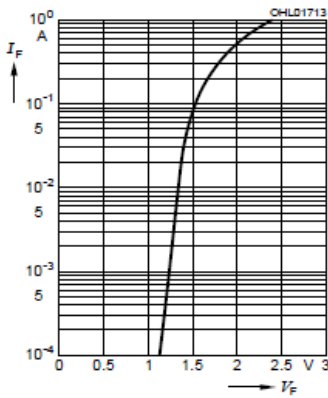
Relative Spectral Emission

$I_{rel} = f(\lambda)$



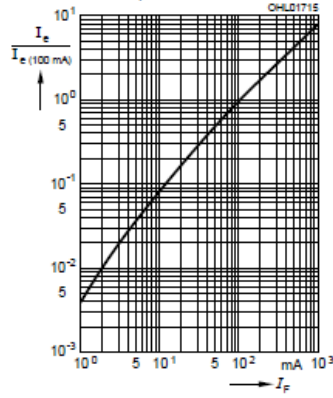
Forward Current $I_F = f(V_F)$

Single pulse, $t_p = 20 \mu s$



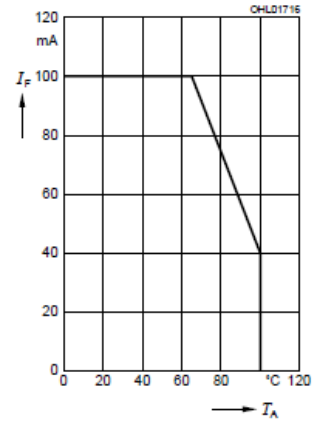
Radiant Intensity $\frac{I_e}{I_e(100 \text{ mA})} = f(I_F)$

Single pulse, $t_p = 20 \mu s$



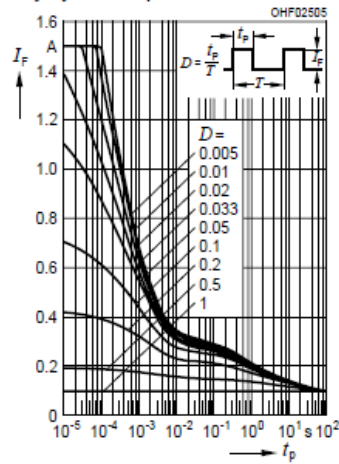
Max. Permissible Forward Current

$I_F = f(T_A), R_{thJA} = 300 \text{ K/W}$

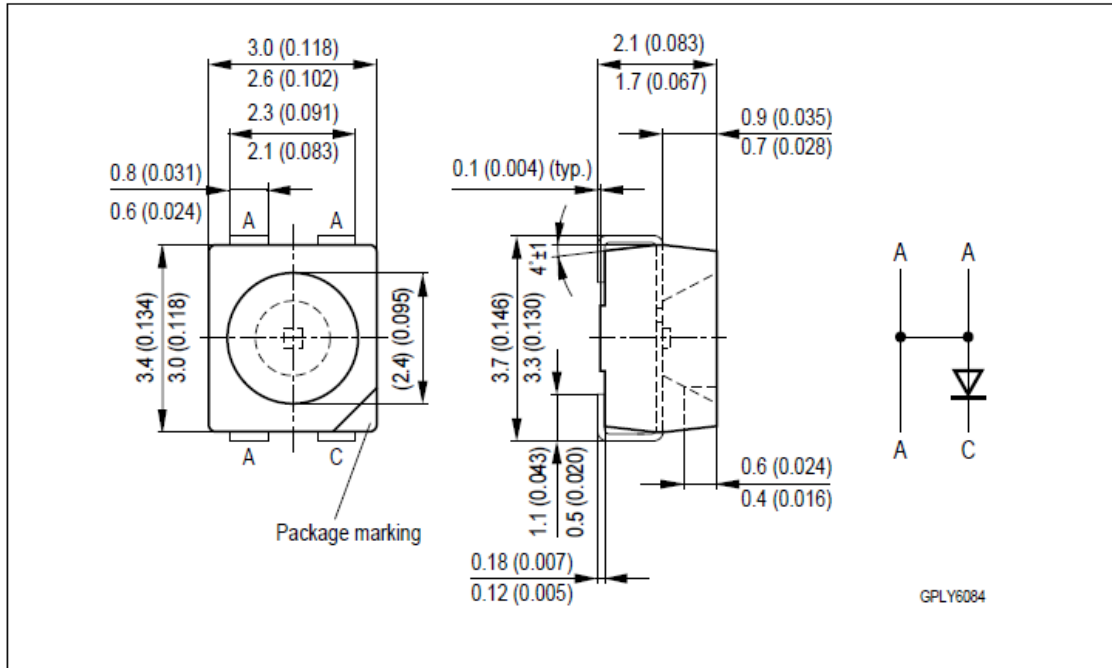


Permissible Pulse Handling Capability

$I_F = f(t, T_A = 25 \text{ °C})$,
duty cycle $D =$ parameter



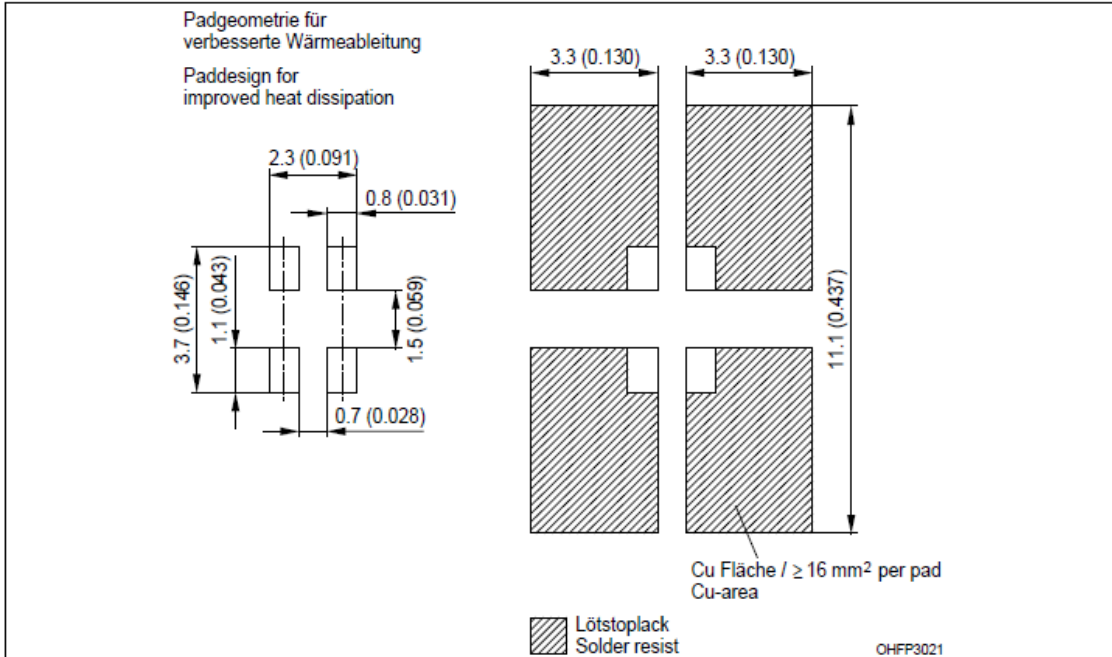
Maßzeichnung
Package Outlines



Gehäuse / Package	Power TOPLED®, klarer Verguss / Power TOPLED®, clear resin
Anschlussbelegung Pin configuration	Kathode: abgeschrägte Ecke Cathode: beveled edge

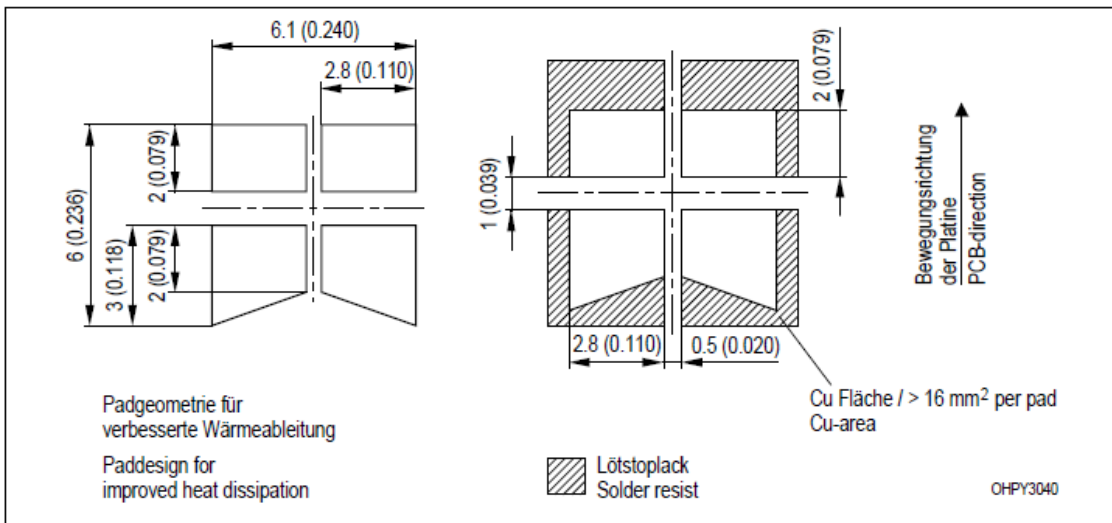
Empfohlenes Lötpad Design
Recommended Solder Pad Design

Reflow Löten
Reflow Soldering



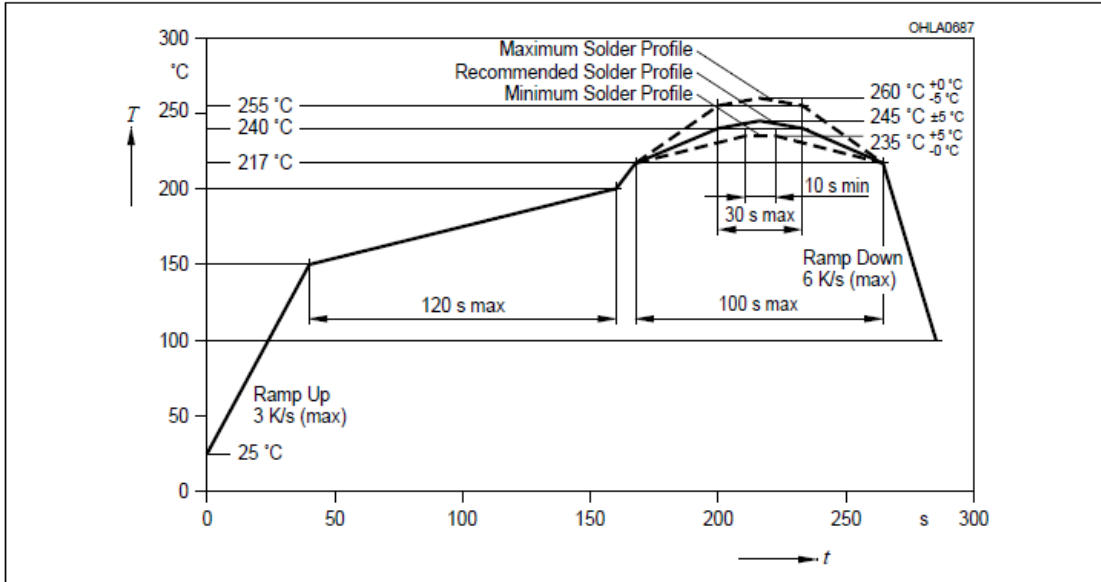
Empfohlenes Lötpad Design
Recommended Solder Pad Design

Wellenlöten TTW
TTW Soldering



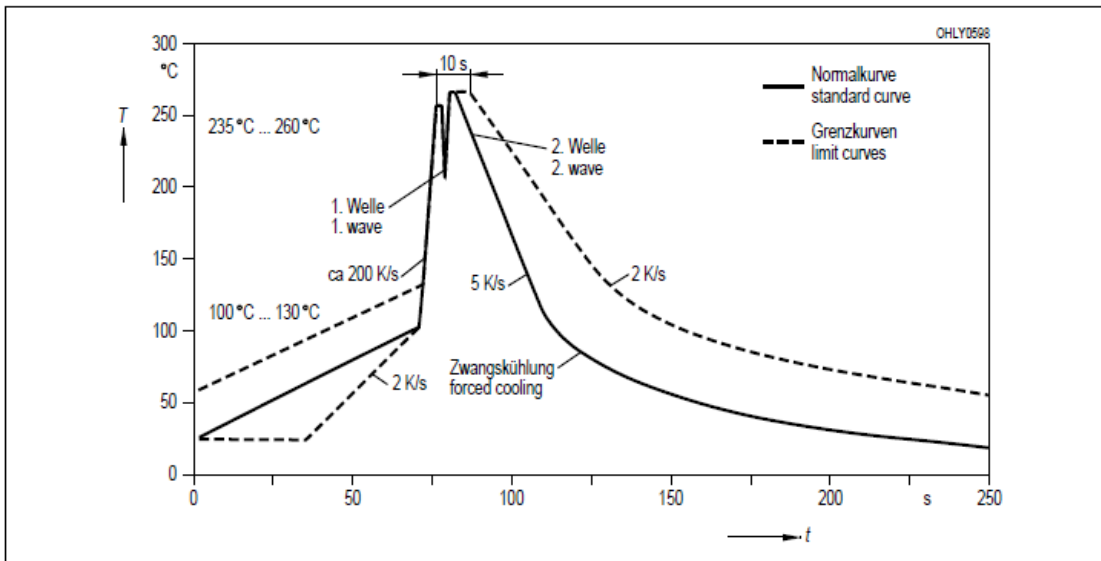
Lötbedingungen
Soldering Conditions
Reflow Lötprofil für bleifreies Löt
Reflow Soldering Profile for lead free soldering

Vorbehandlung nach JEDEC Level 2
 Preconditioning acc. to JEDEC Level 2
 (nach J-STD-020C)
 (acc. to J-STD-020C)



Wellenlöt (TTW)
TTW Soldering

(nach CECC 00802)
 (acc. to CECC 00802)



Published by
OSRAM Opto Semiconductors GmbH
Leibnizstraße 4, D-93055 Regensburg
www.osram-os.com

© All Rights Reserved.

The information describes the type of component and shall not be considered as assured characteristics. Terms of delivery and rights to change design reserved. Due to technical requirements components may contain dangerous substances. For information on the types in question please contact our Sales Organization.

Packing

Please use the recycling operators known to you. We can also help you – get in touch with your nearest sales office. By agreement we will take packing material back, if it is sorted. You must bear the costs of transport. For packing material that is returned to us unsorted or which we are not obliged to accept, we shall have to invoice you for any costs incurred.

Components used in life-support devices or systems must be expressly authorized for such purpose! Critical components ¹, may only be used in life-support devices or systems ² with the express written approval of OSRAM OS.

¹ A critical component is a component used in a life-support device or system whose failure can reasonably be expected to cause the failure of that life-support device or system, or to affect its safety or effectiveness of that device or system.

² Life support devices or systems are intended (a) to be implanted in the human body, or (b) to support and/or maintain and sustain human life. If they fail, it is reasonable to assume that the health of the user may be endangered.

EU RoHS and China RoHS compliant product



此产品符合欧盟 RoHS 指令的要求；

按照中国的相关法规和标准，不含有毒有害物质或元素。

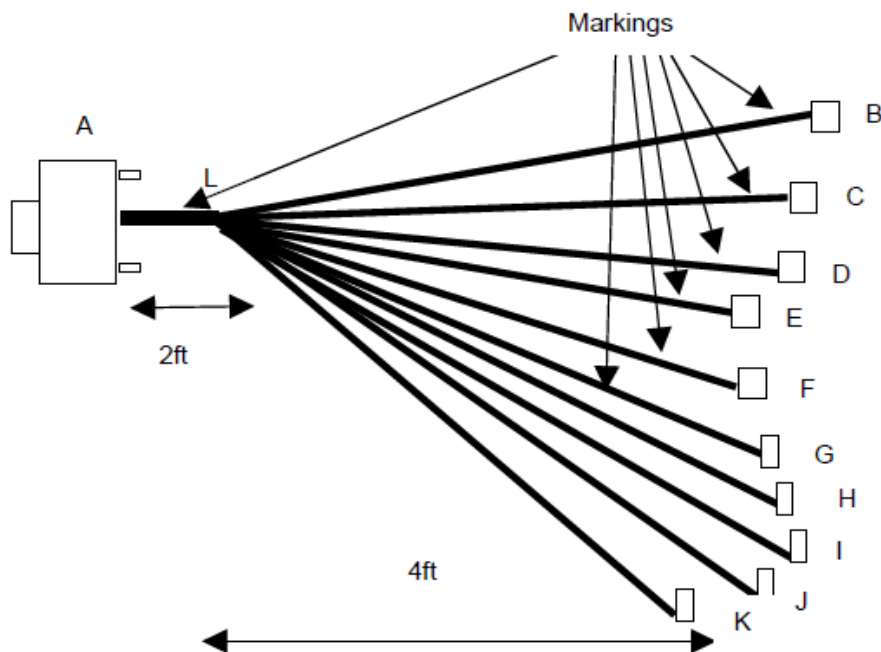
BitFlow, Inc.

Development Cable for Analog board, Virtual Port 1

Part Number CAB-DEV-ANV1

Rev. A

Feb. 25 2007



Connector A is a 62 pin three row D-sub male plug, with metal shell. It has manual screws on the side for mating.

Connectors B,C,D,E,F,G,H,I,J,K are BNC.

The BNC's connect to connector A through coax cable.

Section AL is enclosed in snake skin.

Two inches from connector A, put a marking with a transparent sleeve over it. The marking should be:

**BitFlow, Inc.
CAB-DEV-ANV1**

Two inches from each BNC put a marking with the labels in the table shown below.

A	B	C	D	E	F	G	H	I	J	K	Marking
23 11	wire shield										VIDEO-1
2 6		wire shield									VIDEO-2
1 4			wire shield								VIDEO-3
22 3				wire shield							VIDEO-4
24 43					wire shield						HD
47 44						wire shield					VD
45 48							wire shield				SHOT
25 49								wire shield			TRIGGER
46 52									wire shield		FLASH
26 53										wire shield	WEN



BitFlow
MATLAB Image Acquisition Toolbox:
BitFlow Adaptor Custom Properties

Table of Contents

Introduction.....	3
Device Specific Property Usage.....	3
The Source Object.....	3
Accessor and Modifier Methodology.....	3
BitFlow Adaptor Device Specific Properties.....	4
BFReg.....	4
BFRegVal.....	4
BuffersAllocated.....	4
BuffersToUse.....	5
Exposure.....	5
GPIIn0 to GPIIn4.....	5
GPOut0 to GPOut6.....	5
LineFrame.....	6
TriggerMode.....	6
UseHardwareROI.....	6
Appendix.....	8
I. bf_dec2hex.m.....	8
II. bf_hex2dec.m.....	8

Introduction

Ideal for use in research, education and any other environment desiring rapid application development, the MathWorks, Inc. MATLAB Image Acquisition Toolbox, paired with the Image Processing Toolbox, provides a consistent programmatic framework with which advanced image capture and processing can be achieved. In certain use cases, however, the standard feature set of the Image Acquisition Toolbox can be found inadequate. To accommodate users with more demanding needs, individual Adaptors may provide accessors and modifiers to device specific properties, exposing more of the underlying hardware's full capabilities. It is the express purpose of this document to detail and explain the device specific properties included in the BitFlow, Inc. Adaptor for the MATLAB Image Acquisition Toolbox.

Detailed information on the use of MATLAB and its various toolboxes can be found on the [MathWorks](http://www.mathworks.com) website, including demonstration programs and complete API documentation.

Device Specific Property Usage

The Source Object

Device specific properties are interfaced using the video Source object, a property of the video object, which can be acquired using one of two methods:

```
vidobj = videoinput('bitflow')           % Create the video object
srcobj = get(vidobj, 'Source')           % Acquire the Source object
```

or

```
vidobj = videoinput('bitflow')           % Create the video object
srcobj = vidobj.Source                   % Acquire the Source object
```

Accessor and Modifier Methodology

Three methods are provided by the Image Acquisition Toolbox to access or modify object properties: Verbosely using the `get` and `set` functions, concisely via the dot operator, and visually via the `inspect` function and corresponding GUI dialog. Properties are accessed and modified using the following command operations:

```
get(srcobj)                             % List all available properties
```

```
returned_value = get(srcobj, 'Property') % Verbose accessor
```

```
set(srcobj)                             % List each property and its valid values
```

```
set(srcobj, 'Property')                 % List valid values for the property
```

```
set(srcobj, 'Property', new_value)     % Verbose modifier
```

```
returned_value = srcobj.Property       % Concise accessor
```

```
srcobj.Property = new_value            % Concise modifier
```

Alternatively, a GUI dialog is produced by running `inspect(srcobj)`, which provides an overview of all available properties and their values as of the previous action (dialog open, property modification). This allows non read-only properties to be modified using the mouse and keyboard, for those who prefer such interaction.

BitFlow Adaptor Device Specific Properties

The following are the device specific properties provided by the BitFlow, Inc. MATLAB Image Acquisition Toolbox adaptor. See the [Device Specific Property Usage](#) section for an overview on how device specific properties are used.

BFReg

An enumerated accessor and modifier specifying which BitFlow board register should be read or written by the [BFRegVal](#) property. Each complete register and bit-field sub-register available on the frame grabber will be listed in the enumeration. Details on the registers available for your specific board are listed in the Hardware Reference Manual available at the [Downloads](#) page of the BitFlow website.

Type: Enumeration
Default value: 'con0'
Valid values: Board dependent
Read only: Never

BFRegVal

An integer accessor to and modifier of the BitFlow board register corresponding to the selected [BFReg](#) property. Registers are up to 32-bits long and can be read or written at any time, although not all registers are static, some registers are read-only and some registers are write only. Reference the appropriate BitFlow Hardware Reference Manual – available at the [Downloads](#) page of the BitFlow website – for detailed information regarding your board's registers.

Because the Image Acquisition Toolbox uses 32-bit signed integers, and BitFlow registers are 32-bit unsigned integers, interaction can be complicated for values greater than `0x7fffffff` (decimal value 2,147,483,647). The MATLAB provided `dec2hex` and `hex2dec` functions are inadequate for conversion as both assume unsigned integers are to be used. As an alternative, the `bf_dec2hex.m` and `bf_hex2dec.m` MATLAB script functions are provided in the [Appendix](#), which facilitate conversion between signed and unsigned integers using two's complement and sign inversion, otherwise replicating the `dec2hex` and `hex2dec` functionality.

Type: Integer
Default value: Register dependent or N/A
Valid range: -2147483648 to 2147483647 (complete 32-bit signed integer range)
Read only: Register dependent

BuffersAllocated

This read-only integer indicates how many buffers the adaptor has actually allocated in RAM for the accessed instance of the current Virtual Frame Grabber (VFG). The number of buffers desired for allocation is specified by the [BuffersToUse](#) property. The value returned will be zero if another instance of the same VFG is actively acquiring, or if the buffers could not be allocated (usually resulting from memory size limitations). Otherwise, the value of Buffers Allocated should equal that of [BuffersToUse](#). During run-time, reading [BuffersAllocated](#) will attempt to dynamically allocate the desired number of buffers before returning, and can be used to verify that the VFG is ready for acquisition.

Type: Integer
Default value: N/A

Valid range: 0 ∪ 2 to 50,000
Read only: Always

BuffersToUse

In complement of the *BuffersAllocated* property, this integer value can be read or written at any time, though allocation may not be performed immediately, as the buffer object is shared between each instance of a given Virtual Frame Grabber (VFG), necessitating that allocations only be performed when no other instance of the VFG is acquiring. Additionally, if the specified *BuffersToUse* would exceed available RAM if allocated, no allocation will occur. The *BuffersAllocated* property should generally be checked before attempting to begin acquisition to verify that the desired *BuffersToUse* are actually available and ready to use.

Type: Integer
Default value: 10
Valid range: 2 to 50,000
Read only: Only while this instance is acquiring

Exposure

A double precision floating point value specifying the desired camera exposure period in milliseconds. This property has a limited range and may not work with all cameras; a camera may require special configuration before it will work with the frame grabber specified exposure period. Further, the value of the *Exposure* and *LineFrame* properties are interdependent, as the exposure period should never exceed the line frame period. For additional details, consult to the relevant BitFlow [Hardware Reference Manual](#) for your board and the manufacturer's reference materials for whatever camera is to be used.

Type: Double
Default value: Camera file dependent
Valid range: 0 to 2275.555284
Read only: Never

GPIIn0 to GPIIn4

Integer accessors to the five general purpose inputs. These include both single ended TTL and Differential (LVDS) inputs, with configurations varying from board to board. The only valid values are zero and one, with the former representing an electrical low and the later an electrical high. These properties can be used in conjunction with the general purpose outputs, *GPOut0 to GPOut6*, to interface with external devices.

The general purpose inputs are also accessible via the board registers using the *BFReg* and *BFRegVal* properties. Not every BitFlow frame grabber has all five of these inputs. Consult the relevant BitFlow [Hardware Reference Manual](#) for additional details regarding your board model.

Type: Integer
Default value: Hardware input state determined
Valid range: 0 or 1
Read only: Always

GPOut0 to GPOut6

Integer accessors to and modifiers of the seven general purpose outputs. These include single ended TTL, Differential (LVDS), and Open Collector outputs, with configurations varying from board to board. The only valid values are zero and one, with the former representing an electrical low and the later an electrical high.



These properties can be used in conjunction with the general purpose inputs, *GPIn0 to GPIn4*, to interface with external devices.

The general purpose outputs are also accessible via the board registers using the *BFReg* and *BFRegVal* properties, with advanced configurations possible by setting the *GPOUT0_CON* to *GPOUT6_CON* registers to use the various available signal generating sources. Not every BitFlow frame grabber has all seven of these outputs. Consult the relevant BitFlow [Hardware Reference Manual](#) for additional details regarding your board model.

Type: Integer
Default value: 0
Valid range: 0 or 1
Read only: Never

LineFrame

A double precision floating point value specifying the desired camera line/frame period in milliseconds. The line period is equal to 1/line rate, similarly the frame period is equal to 1/frame rate. This property has a limited range and may not work with all cameras; a camera may require special configuration before it will work with the frame grabber specified line/frame period. Further, the value of the *LineFrame* and *Exposure* properties are interdependent, as the line frame period should never drop below the exposure period. For additional details, consult to the relevant BitFlow [Hardware Reference Manual](#) for your board and the manufacturer's reference materials for whatever camera is to be used.

Type: Double
Default value: Camera file dependent
Valid range: 0.000136 to 2275.555420
Read only: Never

TriggerMode

An enumeration, providing several triggering modes, which control at a low level the mode of acquisition. The default mode is 'Auto', which selects the most likely appropriate mode for the current trigger source, as configured in the IMAQ video device. The other options are described fully in the *TrigMode* portion of the *CiConvTrigModeSet* function documentation, available in the BitFlow [SDK Reference Manual](#). Certain modes are not available on every board, and will generate an error at acquisition start, if selected.

This property is only available for SDK 5.40 and newer.

Type: Enumeration
Default value: 'Auto'
Valid values: 'Auto', 'Free Run', 'One Shot', 'Acquisition Command', 'Acquisition Command Start Stop', 'Continuous Data', 'One Shot Self Triggered', 'One Shot Start A Stop B', 'One Shot Start A Stop A', 'Snap Qualified', 'Continuous Data Qualified', 'One Shot Start A Stop A Level', 'NTG One Shot', 'Triggered Grab'
Read only: Only while acquiring

UseHardwareROI

An enumeration, with only the Boolean 'true' and 'false' options available, which indicates whether the BitFlow board's hardware Region Of Interest (ROI) support should be used (when 'true'), or if the ROI should be extracted via software alone. Hardware ROI has greater throughput and will usually require less memory for the same number of *BuffersAllocated*, but some cameras and configurations do not work well with hardware



ROI, so software is available as a more reliable alternative; hardware ROI is not allowed when using Alta boards, as it is particularly problematic with analog cameras. Try setting UseHardwareROI to 'false' if acquisition becomes problematic when using ROI. Proper setup of a camera's configurations may remedy problems related to hardware ROI.

The acquisition system used when UseHardwareROI is 'true' is actually a mixed-mode hardware/software hybrid, as BitFlow boards do not allow for pixel precise ROI values. When an exact ROI is not possible, the closest-fit larger ROI area is set in hardware and the exact pixel area is extracted in software, mostly preserving the benefits of hardware ROI, while providing all the convenience of software ROI. If ROI acquisition without any software cropping is desired, consult the `CiAgROIset` function documentation in the BitFlow [SDK Reference Manual](#) to determine valid area values for your board, and simply ensure to remain within those constraints.

Type:	Enumeration
Default value:	'true' ('false' for all Alta model boards)
Valid values:	'true', 'false'
Read only:	Only while acquiring (always for all Alta model boards)

Appendix

I. *bf_dec2hex.m*

```
function [ hex_val ] = bf_dec2hex( dec_val )
%BF_DEC2HEX Convert a signed 32-bit int to a hex number
% Regular dec2hex converts unsigned integers to hex strings.
% This function converts signed 32-bit integers to hex strings.

if dec_val < 0
    % If so, perform a sign inversion and
    % two's complement operation.
    dec_val = uint32 (-dec_val); % Invert and convert to an unsigned int.
    dec_val = bitcmp (dec_val) + 1; % Perform the two's complement operation.
end

hex_val = dec2hex (dec_val); % Convert the decimal value to a hex string.

end
```

II. *bf_hex2dec.m*

```
function [ dec_val ] = bf_hex2dec( hex_val )
%BF_HEX2DEC Convert a hex number to a signed 32-bit int
% Regular hex2dec will always produce an unsigned int. This function
% produces the signed 32-bit integer represented by the hex string.

dec_val = hex2dec (hex_val); % Determine the unsigned integer value.
dec_val = uint32 (dec_val); % Cast the value to an unsigned integer container.

if dec_val > 2147483647
    % If so, perform a two's complement and
    % sign inversion. 2147483647 == 0x7fffffff.
    dec_val = bitcmp (dec_val); % Determine the complement.
    dec_val = -int32 (dec_val) - 1; % Perform inversion and 'two' the
end % complement (must be done after
% int32 conversion to prevent overflow;
end % int32 == [-2147483648 2147483647] ).
```

NEWPORT 1830C WITH SILICON DETECTOR

P H O T O N I C S

Model 1830-C

Picowatt Digital Optical Power Meter



The **Model 1830-C** Power Meter is a high-resolution autoranging picoammeter compatible with all of Newport's **818 Series** low-power silicon, germanium and indium gallium arsenide detectors. It is the most popular Newport model used in production testing of fiber optic components.

DC power measurements can be displayed in units of W and dBm on the instrument's 4 1/2 digit annunciator, backlit, wide-angle view LCD, providing wide dynamic range with power sensitivities down to 100 fW and full scale readings up to 2 W, with the OD-3 calibrated optical attenuator. Various detector accessories allow for free-space, as well as for fiber coupled power measurements.

Relative power measurements, in reference to a previously stored value,

can also be performed with the result displayed either as a ratio or in dB.

A built-in beeper, which changes its frequency as a function of incident optical power, can be utilized to optimize optical beam alignment.

RS-232C and IEEE-488 (GPIB) interfaces are both provided as standard features, allowing the remote control of the instrument with a personal computer. Sample LabVIEW drivers are provided upon request.

Additional features include wavelength adjustment in 1 nm steps from the front panel, and an analog output that provides a voltage proportional to the detector current, to be used for recorder or control loop applications.

Key Features

- Compact, full featured, benchtop instrument
- Standard configuration includes both RS-232C and IEEE-488 interfaces
- DC power measurements in the 100 fW–2 W range
- Additional features include large, backlit LCD display, autoranging and an audible tone for alignment optimization

LASER DIODE TESTING

FIBER OPTICS TEST INSTRUMENTATION

POWER METERS & DETECTORS

FIBER ALIGNMENT & ASSEMBLY

LASERS

FIBER OPTIC COMPONENTS

OPTICAL FIBERS & ACCESSORIES

LASER DIODE TESTING

FIBER OPTICS TEST INSTRUMENTATION

POWER METERS & DETECTORS

FIBER ALIGNMENT & ASSEMBLY

LASERS

FIBER OPTIC COMPONENTS

OPTICAL FIBERS & ACCESSORIES

For more details on Newport's low-power detectors and fiber optic attachments compatible with the 1830-C, please see page 141 thru 152.

Call Newport's Application Sales Engineers to help you select the optical detector that best meets your application requirements.

Instrument Specifications

Signal Ranges	Up to 8 decades (dependent on detector type)
Display Type	4.5 digit, annunciator, backlit, wide-angle view LCD
Display Update Rate (ms)	75
Auto-Ranging Time	200 ms (typical)
GPIO Bus Transfer Time	10 ms (typical)
Analog Output	0-2V into 1 MΩ
DC Accuracy	<±0.2% (typical)
Connectors	
Calibration Module	8 pin Sub-mini DIN
Analog Output	0-2V into 1 MΩ
RS-232C	9 pin D-Sub
GPIO	24 Conductor D
Power Requirements	100-120/220-240 VAC, 50/60 Hz
Absolute Maximum Line Current Rating (W x H x D) (mA)	200
Dimension (W x H x D) [in. (mm)]	3.7 (94) x 7.5 (191) x 9.0 (229)
Weight [lb (kg)]	5 (2.3)
Enclosure (W x H x D)	Metal case, painted 7.5 (191) x 9.0 (229) in. (94 x 191 x 229 mm)
Operating Temperature	0°C to +40°C; <70% RH noncondensing
Storage Temperature	-20°C to +60°C; <90% RH noncondensing

System Specifications

The 1830-C is compatible with Newport's Ge, Si and InGaAs detectors, allowing both free-space and fiber pigtailed measurements in the 190-1800 nm range. When using one of these detectors with the 1830-C a calibration module needs to be attached to the detector, assuring the correct reading at any pre-selected wavelength.

Model	818-UV/CM	818-SL/CM	818-F-SL	818-ST/CM	818-IR/CM 818-F-IR	818-IG/CM	818-IS-1
Detector Material	Silicon	Silicon	Silicon	Silicon	Germanium	Indium Gallium Arsenide	InGaAs/Si
Diameter (cm)	1.13	1.13	0.3	1 x 1	0.3	0.3	
Wavelength (nm)	190-1100	400-1100	400-1100	400-1100	780-1800	800-1650	400-1650
Power Range (dBm)	-73 to +23 dBm	-80 to +33 dBm	-80 to +3 dBm	-60 to +33 dBm	-65 to +23 dBm ³⁾	-80 to +23 dBm	-65 to +23 dBm
Display Resolution	0.01 dB or dBm						
Display Resolution (pW)	0.1	0.1	0.1	0.1	10	0.1	0.1
Accuracy ¹⁾	±2%	±2%	±2%	±2%	±3%	±2%	±2.5%
Applicable wavelength range (nm)	200-1100	400-1100	400-1100	400-1100	780-1700	800-1650	400-1650
Linearity	±0.5%						
NEP @ 5 Hz and 1 A/W	fW/√Hz 50	50 fW/√Hz	50 fW/√Hz	3 pW/√Hz	4 pW/√Hz	30 fW/√Hz	3 pW/√Hz ³⁾

1) At calibration temperature maintained to ± 0.2°C, -20 dBm level having 99% encircled energy on detector with no optical attenuator
 2) -70 to +3 dBm for 818-F-IR
 3) 0.01 A/W for the 818-IS-1

Ordering Information

Model	Description
1830-C	Picowatt Digital Optical Power Meter
1830-C-CAL	1830-C with test data and certificate

Safety Hazards Associated with Exposing the Human Eye to Infrared Rays

As applications of biomedical instrumentation utilizing optical methods continue to increase, it is vital to proactively assess the potential safety hazards to direct or indirect users of the proposed device. In this instance, the focus falls into the concern of damage to the human eye (e.g. retina or lens). In this application, the proposed device will utilize infrared rays at 850 nm (outside of the average human visible spectrum). At this specific wavelength, only the following hazards are of concern:

- 1) Thermal injury to the retina of the eye (400 nm to 1400 nm)
- 2) Near-infrared thermal hazards to the lens of the eye (800 nm to 3000 nm)

It is important to note that if the emitting areas of adjacent LED sources are separated by at least 100 milliradians (5.7 degrees), and then the LEDs are considered independent from a retinal hazard standpoint. However, the LEDs are considered in cascade for risk assessment of the cornea and lens, which is the case for the proposed application. Therefore, the amount and positioning of LEDs must be determined before this consideration can be completely assessed. The International Commission on Non-Ionizing Radiation Protection (ICNIRP) and the American Conference of Governmental Industrial Hygienists (ACGIH) have provided exposure limits for near-infrared optical radiation, in addition to providing recommendations regarding the maximum daily exposure to the cornea (listed at 10 mW/cm²) for the proposed wavelength. The duration of exposure plays a critical role in assessing the potential hazards. The threshold set by various organizations is 1,000 seconds or approximately 16.6 minutes. For the purpose of our study, the exposure time to any and all participants or users will not come close to exceeding this threshold. Therefore, equation 1, below, provides the means to calculate the limit for infrared-only exposure:

$$E_{IR-only} = 1.8 * t^{-0.75} \quad [W * cm^{-2}]$$

Equation 1: Exposure limits for infrared-only at exposure durations of less than 1,000 seconds¹

Guidelines have also been instated by the ACGIH and ICNIRP to protect the human retina against retinal thermal hazards, and also “the infrared lens hazards.” Because it has been established that the time of continuous exposure will not exceed the threshold of 1,000 seconds, the ACGIH has provided the limiting radiance for exposure times of less than 810 seconds and all pulsed exposure applications. Equation 2, below, provides the means to calculate limit for NIR applications:

$$L_{NIR} = \Sigma L_{\lambda} * R(\lambda) * \Delta\lambda \leq \frac{3.2}{\alpha * t^{0.25}} \left[\frac{W}{cm^2 * sr^{-1}} \right] \text{ for } t < 810 \text{ s}$$

Equation 2: Limiting Radiance provided by ACGIH for t<810 s and all pulsed exposure²

Therefore, given these equations that govern the exposure limits for the proposed application (in addition to including a 3-fold safety factor), it is determined that the maximum daily exposure time for a human being must not exceed 810 seconds.

APPENDIX C: MATLAB CODE USED FOR IMAGE PROCESSING AND ANALYSIS

The developed MATLAB scripts and functions are shown, below. Various functions were developed for specific purposes. The original script *Pupillometry.m* is used for video acquisition, data collection, and data analysis. The function *pupilProcess.m* is used to process the frame, isolate the pupil and provide the pupil diameter to the calling function. The function *eliminateReflections.m* is used to eliminate unwanted reflections. The function *LSellipse_fit.m* is used to conduct best-ellipse fitting in order to determine the coordinates and diameter of the pupil.

PUPILLOMETRY.M

```
%% Pupillometry.m
%
% Script for data analysis and development
%
% Pupillometry - acquires video and analyzes frames to determine the
% diameter of the pupil. This function requires a video feed from an
```

¹ Mulvey, Exploration of Safety Issues in Eye Tracking. p. 14

² Mulvey, Exploration of Safety Issues in Eye Tracking. p. 15

```

% analog camera which is imported to MATLAB using a BitFLOW Alta-AN1
% frame grabber card.
%
%%Hardware info
% http://www.mathworks.com/help/toolbox/imaq/f9-75080.html
%
%-----

clear all; %Clear workspace
imaqreset; %Reset image acquisition in MATLAB

% ROI values. The original frame should be greater than or equal.
width = 640;
height = 480;

% Set runtime
t = 1;

% Setup the acquisition.
vid = videoinput ('bitflow', 1);
src = vid.Source;
vid.FramesPerTrigger = inf;
vid.ROIPosition = [0 0 width height];

% Acquire a single frame
topframe = getsnapshot (vid);

gcf.DoubleBuffer = 'on';

start (vid); %Start video to acquire frames

i=1; %initialize indexing
area = 100; %initialize feedback

tic;
while toc < t % Set amount of time for test to run
    if (vid.FramesAvailable) %Iterate if a new frame is available

        % Get the most recently acquired frame.
        topframe = peekdata (vid, 1);

        %Thresholding
        if i < 2

            F=medfilt2(F); %median filter to remove noise and preserve
                %edges

            z=imhist(F); %make 256 bin histogram of input image
                %this histogram is used in calculating the
                %threshold value

            thresh=70; %initialize variable value in case
                %histogram analysis fails

            %Calculate threshold value using histogram

            for i=30:256 %skip first 30 intensity values for

```

```

                                %accuracy. When histogram bin value
                                %drops under 40, use that index for
                                %threshold value
        if (z(i) < 30)
            thresh = i;          %set threshold value to loop index
            break;              %break from loop
        end
    end
end

% Clear any other frames.
flushdata (vid);

%Call pupilprocess.m for image processing
[condition, major, minor, phi, x, y] = pupilProcess(topframe,...
    area, thresh);

if (condition == 1)            %Iterate if the frame was properly
                                %processed in pupilProcess.m

    trackdiameter(i) = (major);%Set current diameter to trackdiameter
                                %vector

    % Display percentage change
    if i > 2                    %Skip first frame, no reference data

        %Track percentage change
        change(i) = ((major - trackdiameter(i-1)) / major)*100;

        disp(change(i));        %display percentage change in
                                %workspace

    end                        %end if statement

    area = round((major/2) * (minor/2) * pi);
                                %Feedback for noise elimination

    i=i+1;                    %Increment indexing

end                            %end if statement

% Display the processed frame
figure(1)
imshow (topframe, 'InitialMagnification', 'fit');
                                %plot original input image
hold on
plot_ellipse(major,minor,phi,x,y,'g')
                                %overlay best-fit ellipse on
                                %original image

hold on
plot(x,y,'r*')
                                %overlay calculated center of pupil
                                %on original image

hold off

end                            %end if statement

```

```

    % Pause briefly, so the display will have time to update.
    pause(0.0001);
end

% Cleanup and clear everything.
stop (vid);           %Stop video acquisition
delete (vid);        %Delete video acquisition

-----
                                PUPILPROCESS.M
-----

function [ condition, major_axis, minor_axis, phi, x0, y0 ] = pupilProcess
(frame, pixelArea, thresh)
%Written by: Christopher Walker 01/29/2012
%For use in WPI MQP "Remote Pupillometry"
%Completed in conjunction with Charles Stark Draper Laboratory (Cambridge,
%MA) (CSDL)
%Project members: Christopher Walker, Harold Hovagimian
%Project Advisor: Professor Domhnull Granquist-Fraser
%CSDL Advisor: John Turkovich

% pupilProcess - Given an image and the approximate area of the pupil
% (from the previous iteration), pupilProcess returns the diameter of the
% pupil. The function also returns a condition term, which indicates
% whether the algorithm successfully calculated the pupil size. Also
% returns the major and minor axis, coordinates of the center of the
% ellipse (x0 and y0) and the angle of rotation in radians (phi) with
% respect to the x-axis of the best-fit ellipse.

% Input:
%           frame - a vector of image data
%           pupilArea - a value of the approximate pupil area
%           thresh - a threshold value for image analysis
%
% Output:
%           condition - A term to indicate successful processing of the
%           frame
%           major_axis - magnitude of ellipse longer axis (pupil
%           diameter)
%           minor_axis - magnitude of the shorter axis
%           phi - Angle of rotation in radians with respect to the
%           x-axis
%           x0 - x coordinate of ellipse center
%           y0 - y coordinate of ellipse center
%
%-----

F=frame;           %set frame to variable F.
                  %This sets the input image to
                  %variable F

% F=F(:, :, 1);   %make image grayscale ; only ussful
                  %if input image is color. This is

```

```

%not necessary at this stage,
%because we are input a black/white
%image

[row_size, column_size] = size(F); %get row length and column length
%this is used for indexing of loops
%to ensure that the full image is
%processed and allows for variable
%size images to be input to the
%function

reflection = 0; % Initialize boolean value for
% reflection presence. This tells the
% algorithm that additional processing
% is necessary due to the presence of a
% reflection

maximum = max(max(frame)); % Find maximum intensity of the
% original image

if (maximum > 100) % if the maximum intensity is greater
% than 100, a reflection is present.
% Based on collected data, the maximum
% intensity value of a retroreflected
% pupil is approximately 45.

% Locate the coordinates of the maximum intensity value
[y_max, ind] = max(frame(:));
[x_max, y_max] = ind2sub(size(frame), ind);
reflection = 1; % there is an unwanted reflection
% present in the image (reflection = 1)

end

% Thresholding
bw_70 = (F>thresh); %Threshold image to eliminate only
%pixels with intensity greater than the
%threshold value calculated using
% histogram analysis

bw_labeled = bwlabel(bw_70,8); %8-neighbor analysis, only connected
%components (8-neighbor) are kept

bw_pupil = bwareaopen(bw_labeled,round((pixelArea*0.75)));
%Remove any object containing less than
%x pixels through feedback

se = strel('disk',2); %Create a morphological structuring
%element. The 'disk' creates a flat
%disk-shaped structuring element with a
%radius of 2.

bw_pupil = imclose(bw_pupil,se); %Close all objects in the image space
%detected by the strel function. This
%makes it possible to then fill all
%these objects (next function).

```

```

bw_pupil = imfill(bw_pupil,'holes');%Fill all objects in the image space.
                                     %Makes all values inside these regions
                                     %1

%If a reflection exists, call eliminateReflections.m
if (reflection == 1)
    bw_pupil = eliminateReflections(frame, bw_pupil, thresh, pixelArea);
end

% Edge Detection
edges = edge(bw_pupil,'canny');      %Edge detection using canny window
                                     %This isolates the boundary of the
                                     %pupil to conduct best-ellipse
                                     %fitting. This function sets the edge
                                     %of objects to value 1, all other
                                     %pixels that are not edges are 0

ones = 0;                            %Initialize variable

%Calculate size of the edges array to avoid dynamic allocation
for i=1:row_size
    for j=1:column_size
        if (edges(i,j) == 1)
            ones = ones + 1;
        end
    end
end

Arr=zeros(2,ones);                   % preallocate array

f=1;                                  %loop control variable

%Scan and save coordinates of edges to vectors
for i=1:row_size
    for j=1:column_size
        if (edges(i,j) == 1)
            Arr(1,f) = i;
            Arr(2,f) = j;
            f = f + 1;
        end
    end
end

% 3 coordinates are needed for best-ellipse fitting, this ensures that
% enough coordinates were identified to complete processing without errors
if (size(Arr,2) > 3)

Arr2=Arr';                            %Transpose array for use in
                                     %LSellipse_fit.m

% Complete best ellipse fitting
[major_axis, minor_axis, x0, y0, phi] = LSellipse_fit(Arr2(:,2),Arr2(:,1));

condition = 1;                         %pupilProcess successful (to return to
                                     %main function)
else

```

```

        condition = 0;                                %pupilProcess unsuccessful - ignore
                                                    %data point, set all outputs to 0
        major_axis = 0;                                %Return condition = 0 (unsuccessful to
                                                    %calling function)

        minor_axis = 0;
        x0 = 0;
        y0 = 0;
        phi = 0;
end                                                    %end if statement
end                                                    %End main loop

```

ELIMINATEREFLECTIONS.M

```

function [ bw_pupil ] = eliminateReflections( original, thresholded,
threshold, pixelArea )
%Written by: Christopher Walker 02/26/2012
%For use in WPI MQP "Remote Pupillometry"
%Completed in conjunction with Charles Stark Draper Laboratory (Cambridge,
%MA) (CSDL)
%Project members: Christopher Walker, Harold Hovagimian
%Project Advisor: Professor Domhnull Granquist-Fraser
%CSDL Advisor: John Turkovich

% eliminateReflections - Given an original image, a thresholded image, a
%threshold value, and the approximate area of the pupil, the function
%returns an image vector with all reflections eliminated.

% Input:
%
%         original - original image
%         thresholded - thresholded image
%         threshold - threshold value
%         pixelArea - approximate area of the pupil
%
% Output:
%
%         bw_pupil - image vector with unwanted reflections
%         eliminated. Image of pupil isolated.
%
%-----

% Find connected components in thresholded image. This will determine how
% many total reflections are present (including retroreflected pupil). CC
% is a structure with four fields: Connectivity, ImageSize, NumObjects, and
%PixelIdxList

CC = bwconncomp(thresholded);

%Calculate the region with the maximum intensity (unwanted reflection)
maxRegionIntensity = cell2mat(struct2cell(regionprops(CC, original,
'MaxIntensity')));

%Calculate the region with the minimum intensity

```

```

minRegionIntensity = cell2mat(struct2cell(regionprops(CC, original,
'MinIntensity')));

%Get the region coordinates of all of the regions that indicate a
%reflection
regionCoordinates = struct2cell(regionprops(CC, 'pixelList'));

%Find the minimum intensity value of the region with the maximum intensity
minRegion = min(maxRegionIntensity);

%Find the index of the minimum intensity value of the region with maximum
%intensity
minRegionIndex = find(maxRegionIntensity == min(minRegion),1);

for i=1:(CC.NumObjects)           %For the number of reflection, iterate
    if (i ~= minRegionIndex)      %Iterate only if the region is not the
                                   %region with the minimum maximum
                                   %intensity value (pupil
                                   %retroreflection)

        Coord = cell2mat(regionCoordinates(i));
                                   %Get the coordinates of the region of
                                   %interest for processing

        for h=1:length(Coord)      %Iterate for all coordinates

            y=Coord(h,1);          %Make vector of y values of unwanted
                                   %reflection

            x=Coord(h,2);          %Make vector of x values of unwanted
                                   %reflection

            original(x,y) = 0;      %Set the pixels of the region that was
                                   %determined to be a reflection to 0 in
                                   %the original image

        end                        %end for loop

    end                            %end if statement

end                                %end for loop

% Thresholding
bw_70 = (original>threshold);      %Threshold image to eliminate only
                                   %pixels with intensity greater than the
                                   %threshold value calculated using
                                   % histogram analysis

bw_labeled = bwlabel(bw_70,8);     %8-neighbor analysis, only connected
                                   %components (8-neighbor) are kept

bw_pupil = bwareaopen(bw_labeled,round((pixelArea*0.75)));
                                   %Remove any object containing less than
                                   %x pixels through feedback

```

```

se = strel('disk',2); %Create a morphological structuring
                    %element. The 'disk' creates a flat
                    %disk-shaped structuring element with a
                    %radius of 2.

bw_pupil = imclose(bw_pupil,se); %Close all objects in the image space
                                %detected by the strel function. This
                                %makes it possible to then fill all
                                %these objects (next function).

bw_pupil = imfill(bw_pupil,'holes');%Fill all objects in the image space.
                                %Makes all values inside these regions
                                %1

end %end main loop

```

LSELLIPSE FIT.M

```

function [semimajor_axis, semiminor_axis, x0, y0, phi] = Lsellipse_fit(x, y)
%
% ellipse_fit - Given a set of points (x,y), ellipse_fit returns the
% best-fit ellipse (in the Least Squares sense)
%
% Input:
%
%           x - a vector of x measurements
%           y - a vector of y measurements
%
% Output:
%
%           semimajor_axis - Magnitude of ellipse longer axis
%           semiminor_axis - Magnitude of ellipse shorter axis
%           x0 - x coordinate of ellipse center
%           y0 - y coordinate of ellipse center
%           phi - Angle of rotation in radians with respect to
%                the x-axis
%
% Algorithm used:
%
% Given the quadratic form of an ellipse:
%
%           a*x^2 + 2*b*x*y + c*y^2 + 2*d*x + 2*f*y + g = 0   (1)
%
% we need to find the best (in the Least Square sense) parameters
a,b,c,d,f,g.
% To transform this into the usual way in which such estimation problems are
presented,
% divide both sides of equation (1) by a and then move x^2 to the
% other side. This gives us:
%
%           2*b'*x*y + c'*y^2 + 2*d'*x + 2*f'*y + g' = -x^2   (2)
%

```

```

% where the primed parameters are the original ones divided by a.
% Now the usual estimation technique is used where the problem is
% presented as:
%
%  $M * p = b$ , where  $M = [2*x*y \ y^2 \ 2*x \ 2*y \ ones(size(x))]$ ,
%  $p = [b \ c \ d \ e \ f \ g]$ , and  $b = -x^2$ . We seek the vector  $p$ , given by:
%
%  $p = pseudoinverse(M) * b$ .
%
% From here on I used formulas (19) - (24) in Wolfram Mathworld:
% http://mathworld.wolfram.com/Ellipse.html
%
% Programmed by: Tal Hendel <thendel@tx.technion.ac.il>
% Faculty of Biomedical Engineering, Technion- Israel Institute of Technology
% 12-Dec-2008
%
% Shared program obtained through the Mathworks MATLAB function file
% sharing online library. Used in pupilProcess.m and called by
% Pupillometry.m, which are files used in the "Remote Pupillometry Project"
% conducted by:
%
% Christopher Walker
% Harold Hovagimian
%
% Project completed by Worcester Polytechnic Institute in conjunction with
% Charles Stark Draper Laboratory
%
%-----

x = x(:);
y = y(:);

%Construct M
M = [2*x.*y y.^2 2*x 2*y ones(size(x))];

% Multiply (-X.^2) by pseudoinverse(M)
e = M\(-x.^2);

%Extract parameters from vector e
a = 1;
b = e(1);
c = e(2);
d = e(3);
f = e(4);
g = e(5);

%Use Formulas from Mathworld to find semimajor_axis, semiminor_axis, x0, y0
%, and phi

delta = b^2-a*c;

x0 = (c*d - b*f)/delta;
y0 = (a*f - b*d)/delta;

phi = 0.5 * acot((c-a)/(2*b));

```

```
nom = 2 * (a*f^2 + c*d^2 + g*b^2 - 2*b*d*f - a*c*g);
s = sqrt(1 + (4*b^2)/(a-c)^2);

a_prime = sqrt(nom/(delta* ((c-a)*s - (c+a))));
b_prime = sqrt(nom/(delta* ((a-c)*s - (c+a))));

semimajor_axis = max(a_prime, b_prime);
semiminor_axis = min(a_prime, b_prime);

if (a_prime < b_prime)
    phi = pi/2 - phi;
end
```

APPENDIX D: MATLAB CODE PROFILES

During the analysis of the frame rate of the system, it was necessary to examine the MATLAB profiles of the functions called during processing. This technique can provide information regarding specific lines or functions which are consuming large amounts of time. With this information, changes and alterations can be made to improve the speed of the MATLAB code. Profiles on *pupilProcess.m*, *eliminateReflections.m*, and *LSellipse_fit.m* are provided, below.

PUPILPROCESS.M

pupilProcess (1 call, 0.425 sec)

Generated 17-Mar-2012 17:32:54 using cpu time.

function in file C:\Users\Public\Documents\Pupil_Shared\MMU2_Iris_Database\pupilProcess.m

[Copy to new window for comparing multiple runs](#)

Refresh

- Show parent functions
 Show busy lines
 Show child functions
 Show Code Analyzer results
 Show file coverage
 Show function listing

Parents (calling functions)

No parent

Lines where the most time was spent

Line Number	Code	Calls	Total Time	% Time	Time Plot
94	<code>edges = edge(bw_pupil, 'canny')...</code>	1	0.107 s	25.2%	
90	<code>bw_pupil = eliminateReflection...</code>	1	0.066 s	15.5%	
103	<code>if (edges(i,j) == 1)</code>	307200	0.040 s	9.4%	
122	<code>end</code>	307200	0.038 s	8.9%	
117	<code>if (edges(i,j) == 1)</code>	307200	0.037 s	8.7%	
All other lines			0.137 s	32.2%	
Totals			0.425 s	100%	

Children (called functions)

Function Name	Function Type	Calls	Total Time	% Time	Time Plot
edge	function	1	0.107 s	25.2%	
eliminateReflections	function	1	0.066 s	15.5%	
imclose	function	1	0.022 s	5.2%	
medfilt2	function	1	0.019 s	4.5%	
imfill	function	1	0.013 s	3.1%	
bwareaopen	function	1	0.013 s	3.1%	
strel>strel.strel	subfunction	1	0.011 s	2.6%	
imhist	function	1	0.006 s	1.4%	
bwlabel	function	1	0.003 s	0.7%	
LSellipse_fit	function	1	0.002 s	0.5%	
ind2sub	function	1	0.002 s	0.5%	
Self time (built-ins, overhead, etc.)			0.161 s	37.9%	
Totals			0.425 s	100%	

ELIMINATEREFLECTIONS.M

eliminateReflections (1 call, 0.116 sec)

Generated 17-Mar-2012 17:40:08 using cpu time.

function in file <C:\Users\Public\Documents\Pupil Shared\MMU2 Iris Database\eliminateReflections.m>
[Copy to new window for comparing multiple runs](#)

Refresh

- Show parent functions
 Show busy lines
 Show child functions
 Show Code Analyzer results
 Show file coverage
 Show function listing

Parents (calling functions)

No parent

Lines where the most time was spent

Line Number	Code	Calls	Total Time	% Time	Time Plot
34	maxRegionIntensity = cell2mat(...	1	0.037 s	31.9%	
98	bw_pupil = imclose(bw_pupil,se...	1	0.024 s	20.7%	
103	bw_pupil = imfill(bw_pupil,'ho...	1	0.017 s	14.7%	
89	bw_pupil = bwareaopen(bw_label...	1	0.012 s	10.3%	
93	se = strel('disk',2); ...	1	0.008 s	6.9%	
All other lines			0.018 s	15.5%	
Totals			0.116 s	100%	

Children (called functions)

Function Name	Function Type	Calls	Total Time	% Time	Time Plot
regionprops	function	3	0.043 s	37.1%	
imclose	function	1	0.024 s	20.7%	
imfill	function	1	0.017 s	14.7%	
bwareaopen	function	1	0.012 s	10.3%	
strel>strel.strel	subfunction	1	0.008 s	6.9%	
bwconncomp	function	1	0.005 s	4.3%	
cell2mat	function	3	0.003 s	2.6%	
bwlabel	function	1	0.002 s	1.7%	
Self time (built-ins, overhead, etc.)			0.002 s	1.7%	
Totals			0.116 s	100%	

LSELLIPSE_FIT.M

LSellipse_fit (1 call, 0.003 sec)

Generated 17-Mar-2012 17:45:58 using cpu time.

function in file C:\Users\Public\Documents\Pupil Shared\MMU2 Iris Database\LSellipse_fit.m

[Copy to new window for comparing multiple runs](#)

Refresh

- Show parent functions Show busy lines Show child functions
 Show Code Analyzer results Show file coverage Show function listing

Parents (calling functions)

No parent

Lines where the most time was spent

Line Number	Code	Calls	Total Time	% Time	Time Plot
90	nom = 2 * (a*f^2 + c*d^2 + g*b...	1	0.001 s	33.3%	
88	phi = 0.5 * acot((c-a)/(2*b));	1	0.001 s	33.3%	
102	end	1	0 s	0%	
101	phi = pi/2 - phi;	1	0 s	0%	
100	if (a_prime < b_prime)	1	0 s	0%	
All other lines			0.001 s	33.3%	
Totals			0.003 s	100%	

Children (called functions)

No children